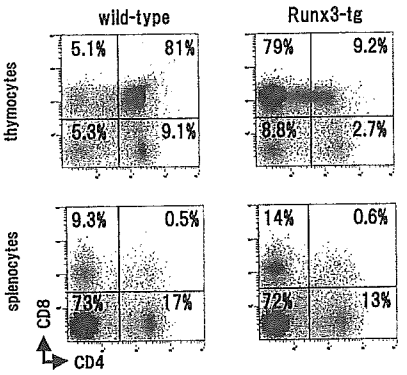

FIGURE 2. Flow cytometrical analysis of thymocytes and splenocytes. The cells from wild-type and *Runx3*-transgenic mice were stained for CD4 and CD8 and processed for flow cytometry. Numbers given in the individual quadrants indicate the percentage of cells of each type.

region under the control of the proximal *Lck* gene promoter. This promoter is known to be active in immature as well as mature T cells and in thymic as well as peripheral T cells (16). Transgenic mouse lines were established and the expression of Runx3 protein was examined by immunoblot analysis using an anti-Runx Ab (Fig. 1*A*). The 52-kDa Runx3 band was clearly detected in the extract of both $CD4^+8^-$ and $CD4^-8^+$ fractions, which were prepared from transgenic thymi as well as spleens. The endogenous Runx3 was also detected in the wild-type, $CD4^-8^+$ thymocytes and splenocytes but to a much lesser degree compared with the transgenic cells. Thus, the magnitude of Runx3 overexpression in the transgenic vs wild-type cells was roughly 5-fold in the case of thymi and 3-fold in the case of spleens. A very faint band seen in the $CD4^+8^-$ wild-type cells represents the nonspecific reaction of the Ab, because the band was not abolished by the preabsorption of the Ab with the Ag peptide. The endogenous Runx1 protein of 56 kDa was detected in all the fractions tested.

We assessed the contribution of overexpressed Runx3 to the Runx-specific DNA binding activity using EMSA (Fig. 1*B*). The endogenous activity detected in a thymocyte extract from wild-type mice was mainly due to the Runx1 protein. The extract from transgenic thymocytes gave rise to a band that migrated slightly faster, reflecting the smaller size of the Runx3 protein compared Runx1 (52 vs 56 kDa). Addition of an anti-HA Ab supershifted the band of the transgenic, HA-tagged Runx3 but not that of the endogenous Runx1 protein. Similar results were seen in the extracts of splenocytes, although the band intensity was much weaker due to the presence of other than the T cells.

The percentage of $CD4^-8^+$ cells increases and the percentage of $CD4^+8^+$ and $CD4^+8^-$ cells simultaneously decreases in the Runx3-transgenic thymus

After confirming the protein expression of transgenic Runx3, we evaluated its effect on T cell differentiation. Flow cytometry was used to analyze CD4 and CD8 in thymocytes and splenocytes (Fig. 2). In the *Runx3*-transgenic thymi, the percentage of $CD4^-8^+$ cells

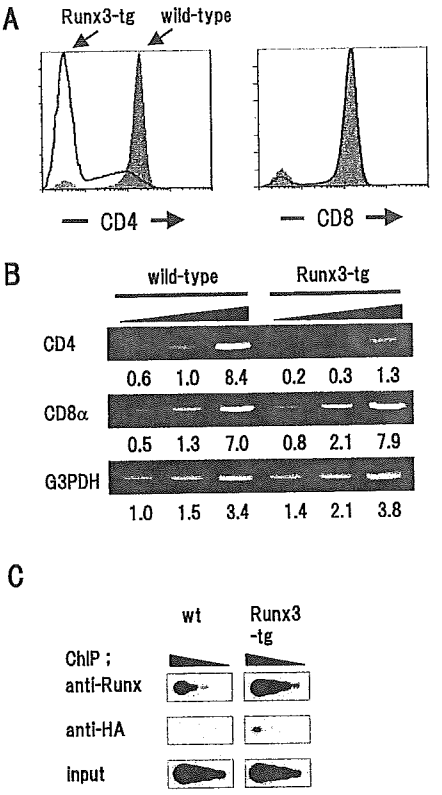

FIGURE 3. CD4 and CD8 expression in the wild-type and *Runx3*-transgenic cells. *A*, Thymocytes stained for CD4 or CD8 were analyzed for their fluorescence intensity. The shaded peak represents the wild-type cells, whereas the open peak represents the *Runx3*-transgenic cells. *B*, Semiquantitative RT-PCR analysis of *CD4*, *CD8α*, and *G3PDH* transcripts. An increasing amount of cDNA synthesized from the wild-type and *Runx3*-transgenic thymocytes was used for PCR. The relative amounts of PCR products were measured and are shown as numbers below the gels. The *G3PDH* product obtained for the least amount of wild-type cDNA was taken to be 1.0. *C*, Chromatin immunoprecipitation analysis. A chromatin fraction prepared from the wild-type and *Runx3*-transgenic thymocytes was immunoprecipitated by an anti-Runx or anti-HA Ab, respectively. DNA was purified from the precipitates, and an increasing amount of DNA fraction was processed as a template for PCR. The PCR products were detected by a *CD4* silencer-specific oligonucleotide. Input means a DNA fraction that was present in the chromatin fraction before immunoprecipitation.

increased to 80% of the total population, whereas the percentage of $CD4^+8^+$ cells decreased to only 9%; the percentage of $CD4^+8^-$ cells also decreased substantially. The unusual profile of CD4 and CD8 expression in the transgenic thymocytes was reflected in the transgenic splenocytes as well. In the transgenic spleen, the percentage of $CD4^-8^+$ cells was higher than that of $CD4^+8^-$ cells, whereas the opposite was true in the wild-type spleen.

We counted the number of cells that were recovered from the thymi and spleens of several individual adult mice (Table I). The number of transgenic thymocytes was ~60% of that of wild-type

Table I. *The numbers and percentages of SP cells in wild-type and Runx3-transgenic thymi and spleens*[a]

	Thymus				Spleen		
	Total cells ($\times 10^8$)	$CD4^+8^+$ (%)	$CD4^+8^-$ (%)	$CD4^-8^+$ (%)	Total cells ($\times 10^8$)	$CD4^+8^-$ (%)	$CD4^-8^+$ (%)
Wild type (n = 9)	2.20 ± 0.67	80.8 ± 1.5	8.73 ± 0.51	5.36 ± 0.63	1.13 ± 0.52	15.5 ± 5.26	7.56 ± 2.38
Runx3-transgenic (n = 9)	1.33 ± 0.46	10.9 ± 1.7	2.21 ± 0.29	78.3 ± 1.7	0.84 ± 0.35	8.73 ± 3.92	10.55 ± 3.85

[a] The means and SD are presented. n, The number of individual mice examined.

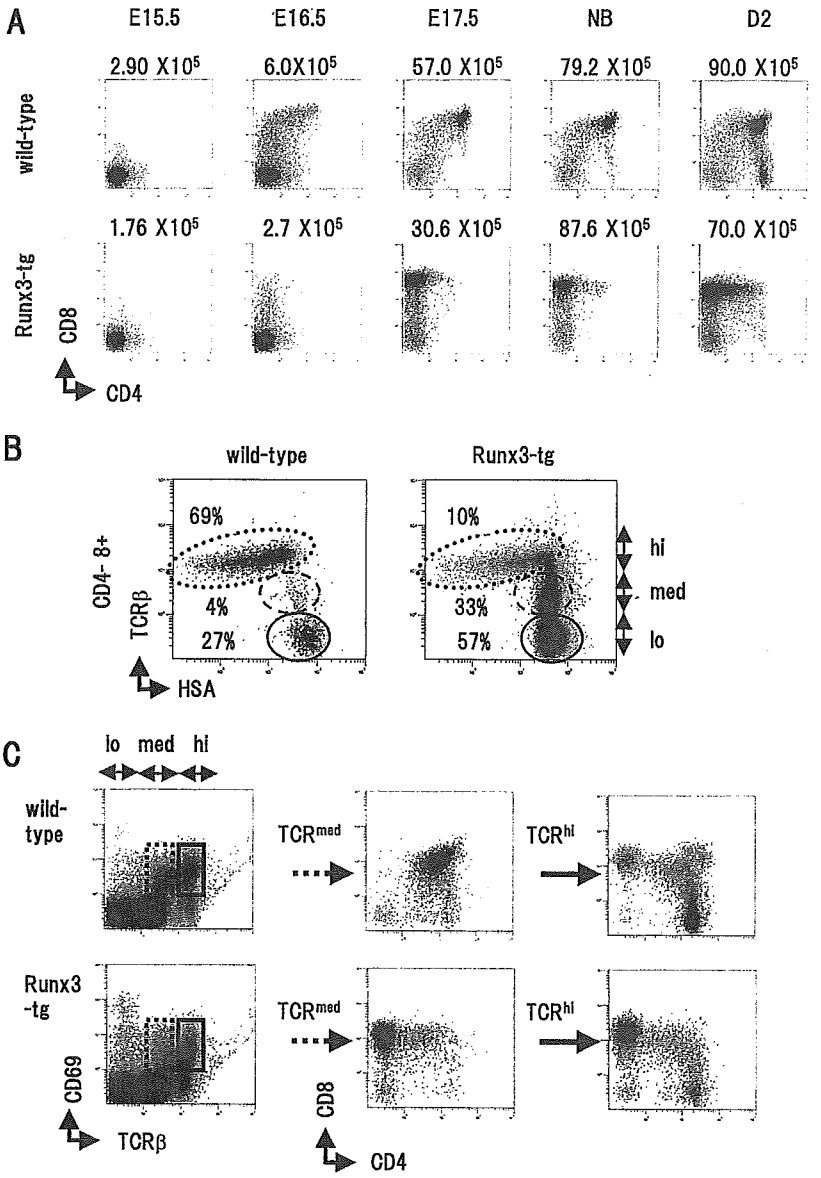

FIGURE 4. Different subpopulations exist in the $CD4^-8^+$ fractions from wild-type and *Runx3*-transgenic thymus. *A*, Ontogeny of thymocyte development. Thymocytes were prepared from wild-type and *Runx3*-transgenic mice at E15.5, E16.5, E17.5, birth (NB), and 2 days after birth (D2). The cells were stained for CD4 and CD8 and processed for flow cytometry. The numbers above each panel indicate the number of cells recovered. *B*, The wild-type and *Runx3*-transgenic thymocytes from adult mice were processed for four-color flow cytometrical analysis. The $CD4^-CD8^+$ fractions were further analyzed for their TCR and HSA expression profiles. The level of TCR expression was classified into three stages (lo, med, and hi), as indicated. The numbers represent the percentages of each subpopulation in the $CD4^-8^+$ fraction. *C*, CD69 and TCR expression profiles in differentiating thymocytes. The wild-type and *Runx3*-transgenic thymocytes were processed for four-color flow cytometry. The cells were first screened for their CD69 and TCR expression profiles. The $TCR^{med}CD69^+$ (broken boxes) and $TCR^{high}CD69^+$ fractions (solid boxes) were further analyzed for their CD4 and CD8 expression profiles.

thymocytes. As a result, the number of cells in the $CD4^-8^+$ fraction was higher, and the number in the $CD4^+8^+$ and $CD4^+8^-$ fractions was lower, in the transgenic thymi compared with the wild-type thymi. The total number of splenocytes did not differ significantly between the two genotypes.

Decrease in the CD4 expression in the Runx3-transgenic thymocytes

The increase in the $CD4^-8^+$ fraction in the *Runx3*-transgenic thymus could be due either to an increase in CD8 expression or a decrease in CD4 expression. To distinguish these two possibilities, the CD8 and CD4 expression profiles were displayed for the wild-type and the *Runx3*-transgenic thymocytes (Fig. 3*A*). The relative ratios of $CD8^-$ and $CD8^+$ cells were not different between the two genotypes. In contrast, the number of $CD4^-$ cells was greatly increased and the number of $CD4^+$ cells was decreased in the transgenic thymus compared with the wild-type thymus.

We also performed a semiquantitative RT-PCR analysis of *CD4* and *CD8* transcripts (Fig. 3*B*). RNA was prepared from the thymocytes, and increasing amounts of the cDNAs were processed for PCR. Although the relative amount of *CD8* transcript did not differ significantly between the two types of cells, many fewer *CD4* transcripts were present in the *Runx3*-transgenic thymocytes compared with the wild-type cells.

The *CD4* silencer is proposed to be a main target by a Runx3 transcription factor (13, 14). We checked this by chromatin immunoprecipitation analysis (Fig. 3*C*). An increasing amount of chromatin fraction-derived DNA that was precipitated by the anti-Runx or anti-HA Ab was processed for PCR and hybridized by a *CD4* silencer-specific oligonucleotide. Both Abs precipitated a significantly greater amount of *CD4* silencer sequence from the *Runx3*-transgenic thymocytes compared with the wild-type cells. The results in Fig. 3 thus suggest that the phenotypic alteration seen in the transgenic thymocytes in Fig. 2 can be at least partly explained by the down-regulation of *CD4* expression.

The increased $CD4^-8^+$ fraction of transgenic thymocytes includes immature, premature, and mature subpopulations

We next characterized in detail the $CD4^-8^+$ fraction of transgenic thymocytes. As described below, this fraction was found to contain three different subpopulations: immature, premature, and mature cells.

The first subpopulation in the $CD4^-8^+$ fraction was recognized as immature single-positive (ISP) cells, which can be easily seen by following the ontogeny of thymocyte development (Fig. 4*A*). In wild-type thymus, only $CD4^-8^-$ cells were detected at embryonic day (E)15.5. $CD4^-8^+$ ISP cells transiently appeared at E16.5, $CD4^+8^+$ cells at E17.5, and $CD4^+8^-$ cells at day 2 after birth. In the *Runx3*-transgenic thymus, immature $CD4^-8^+$ cells first appeared at E16.5 and remained as the main population until after birth. The persistence of ISP cells is probably due to the down-regulation of *CD4* by Runx3. This *CD4* repression appeared to be partial, because some $CD4^+8^+$ and $CD4^+8^-$ cells emerged at day 2 after birth in transgenic mice.

Immature $CD4^-8^+$ cells were also prominent in thymi from adult transgenic mice. To further characterize this population, flow cytometry was first used to select the $CD4^-8^+$ fraction of the thymocytes, and then the expression profiles of TCRβ (hereafter TCR) and heat-stable Ag (HSA) were displayed for this fraction (Fig. 4*B*). The immature $TCR^{low}HSA^{high}$ fraction made up 27% of the wild-type and 57% of the transgenic $CD4^-8^+$ thymocytes. Therefore, overexpression of Runx3 increased the number of ISP cells.

Another characteristic of the transgenic $CD4^-8^+$ fraction was the presence of an aberrant $TCR^{med}HSA^{high}$ subpopulation that was not as apparent in the wild-type fraction (33 vs 4%; Fig. 4*B*). The medium degree of TCR expression indicates that this second subpopulation should be categorized as representing the premature DP stage rather than the ISP stage. We further confirmed this point by staining the thymocytes with CD69, a marker of positive selection (Fig. 4*C*). In the case of wild-type cells, the $TCR^{med}CD69^+$ cells exhibited a $CD4^+8^+$ phenotype, whereas the $TCR^{high}CD69^+$ exhibited both the $CD4^+8^-$ and $CD4^-8^+$ phenotypes. The $TCR^{med}CD69^+$ population could also be detected in the transgenic thymus, but the apparent phenotype of this population was $CD4^-8^+$, not $CD4^+8^+$. The $CD4^-8^+$ fraction persisting in the developing transgenic thymus (Fig. 4*A*) may contain these TCR^{med} cells as well. Thus, the second subpopulation can be summarized as the premature, "CD4-repressed DP" cells.

The transgenic $CD4^-8^+$ fraction also contained a third subpopulation of mature, $TCR^{high}HSA^{low}$ cells (see 10% in Fig. 4*B*). We next evaluated the effect of Runx3 overexpression on these mature $CD4^-8^+$ cells. To do so, we first obtained a TCR expression profile for the total thymocyte population (Fig. 5*A*). Both the wild-type and *Runx3*-transgenic thymi contained TCR^{low}, TCR^{med}, and TCR^{high} subpopulations to a comparable degree. Because the TCR^{high} subpopulation corresponds to mature cells, overexpression of Runx3 did not appear to arrest or block thymocyte differentiation. We gated the TCR^{high} subpopulation and then displayed the CD4/8 profile (Fig. 5*B*). In the TCR^{high} thymocytes from the wild-type, the percentage of $CD4^-8^+$ cells was one-third that of $CD4^+8^-$ cells, whereas in the transgenic TCR^{high} thymocytes, the percentage of $CD4^-8^+$ cells was three times that of $CD4^+8^-$ cells. We also counted the cell numbers constituting each fraction and found that the absolute number of $CD4^-8^+TCR^{high}$ cells in the transgenic thymi was approximately twice that in the wild-type thymi.

To further verify the differentiation stage of the apparently mature $CD4^-8^+$ cells that were generated in *Runx3*-transgenic thymi, we examined the marker expression in the HSA^{low} cells by RT-PCR analysis (Fig. 5*C*). A transcript of *perforin1*, a $CD4^-8^+$ marker (21), was clearly detected in the wild-type as well as *Runx3*-transgenic $CD4^-8^+$ cells, but detected only in a subtle amount in the $CD4^+8^-$ cells of both genotypes. In contrast, a transcript of *GATA3*, a $CD4^+8^-$ marker (21), was expressed more abundantly in the $CD4^+8^-$ cells than in the $CD4^-8^+$ cells irrespective of genotypes of cells. The results in Fig. 5 indicate that the overexpressed Runx3 in fact promoted the differentiation and maturation of thymocytes toward the CD8 lineage.

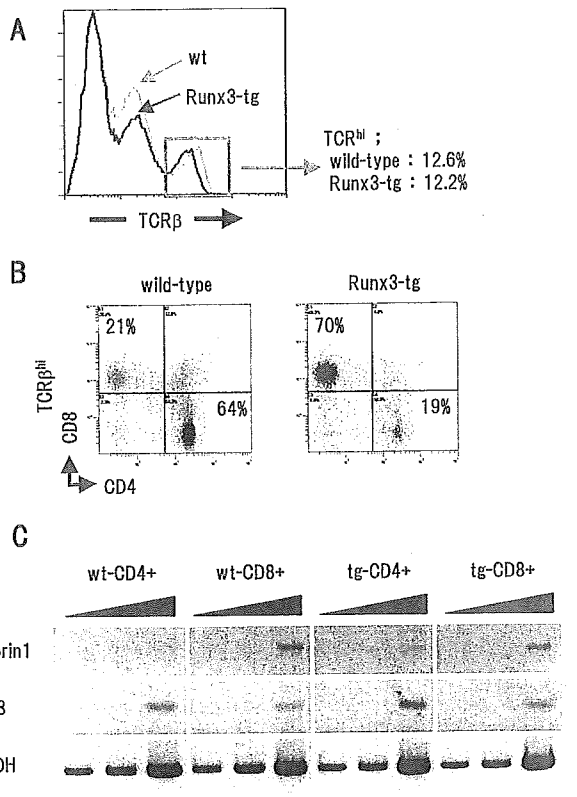

FIGURE 5. Effect of the *Runx3* transgene on the differentiation of mature, TCR^{high} cells. *A*, The thymocytes from wild-type and *Runx3*-transgenic mice were stained for TCR, and their expression profiles were analyzed. The cells were classified into three subpopulations: TCR^{low}, TCR^{med}, and TCR^{high}. *B*, The wild-type and *Runx3*-transgenic thymocytes were processed for three-color flow cytometrical analysis. The mature, TCR^{high} subpopulation was selected, and its CD8 and CD4 expression profile was analyzed. The numbers in the individual quadrants indicate the percentage of cells of each type. *C*, Semiquantitative RT-PCR analysis of *perforin1*, *GATA3*, and *G3PDH* transcripts. RNA was isolated from the $CD4^+8^-HSA^{low}$ and $CD4^-8^+HSA^{low}$ thymocytes' fractions and converted to cDNA. An increasing amount of cDNA synthesized from the wild-type and *Runx3*-transgenic cells, respectively, was processed for PCR.

The mature $CD4^-8^+$ cells are released into periphery of Runx3-transgenic mice

Promotion of thymocyte differentiation toward the CD8 lineage by Runx3 was also reflected in the cell composition in the spleen (Fig. 6, *A* and *B*). Among the $TCR^{high}HSA^{low}$ mature T cells, the ratio of $CD4^-8^+$ cells to $CD4^+8^-$ cells was 0.5 in the spleens from the wild type, but was 1.4 in the transgenic splenocytes.

We wondered whether the increase in mature $CD8^+$ cells reflected the preferential expansion of a specific repertoire of TCR. We therefore examined the usage of Vβ regions by the $TCR^{high}CD8^+$ splenocytes using flow cytometry (Fig. 6*C*). The pattern of the Vβ repertoire was essentially similar between the transgenic and wild-type cells. Therefore, in the *Runx3*-transgenic mice, apparently normal, multiclonal, mature $CD8^+$ cells were generated in the thymus and released into periphery as in the wild-type mice.

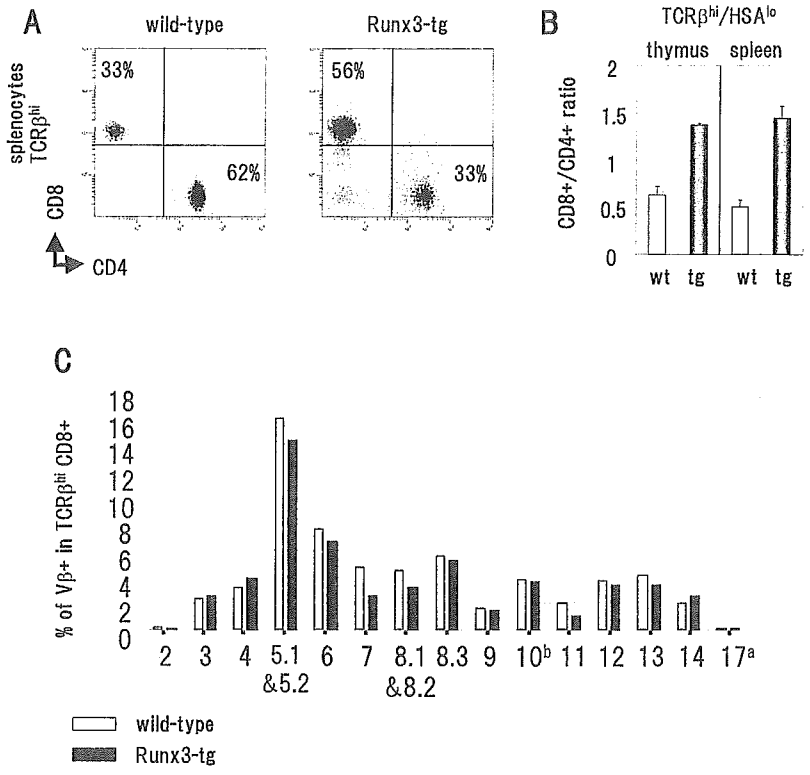

FIGURE 6. Effect of the *Runx3*-transgene on splenic T lymphocytes. *A*, The wild-type and *Runx3*-transgenic splenocytes were processed for three-color flow cytometrical analysis. The mature TCR^{high} subpopulation was selected, and its CD8 and CD4 expression profile was analyzed. The numbers in the individual quadrants indicate the percentage of cells of each type. *B*, The cell number ratios of $TCR^{high}HSA^{low}CD4^{-}8^{+}$ cells to $TCR^{high}HSA^{low}CD4^{+}8^{-}$ cells in the wild-type and *Runx3*-transgenic thymus and spleen. *C*, The Vβ repertoire used by the TCRs of splenic $CD4^{-}8^{+}$ cells. Wild-type (□) and *Runx3*-transgenic (■) cells were stained by an Ab mixture against various Vβ segments and processed for flow cytometrical analysis.

Overexpression of Runx3 can drive originally CD4-oriented thymocytes toward the CD8 lineage

The results shown in Figs. 5 and 6 indicate that the overexpressed Runx3 can drive thymocytes to select and mature along the CD8 lineage. We then examined whether this effect of Runx3 is dependent on the TCR signaling elicited from proper MHC interactions. The *TCR* transgene, which is restricted to MHC class II, was introduced into *Runx3* transgenic mice (Fig. 7*A*). Thymi from *TCR* single-transgenic mice showed a skew of cell differentiation to the CD4 lineage (33% $CD4^{+}8^{-}$ compared with 3.6% $CD4^{-}8^{+}$). In contrast, in the *TCR* and *Runx3* double-transgenic thymi, the $CD4^{-}8^{+}$ cells constituted the major population (73%), just as in the case of *Runx3*-single-transgenic thymi. When only the mature cells were selected by gating the HSA^{low} fraction (and by gating the transgene-specific TCR^{high} fraction as well (data not shown)), it was clear that the *Runx3* transgene switched the differentiation of class II-restricted cells to the CD8 lineage.

We further confirmed the cell-autonomous activity of Runx3 by altering the MHC background. The $\beta_2 m$ (−/−), class I-deficient thymus provides an environment unfavorable for the selection of $CD4^{-}8^{+}$ cells (Fig. 7*B*). In the TCR^{high} fraction, 90% of wild-type thymocytes were $CD4^{+}8^{-}$ cells. In contrast, the *Runx3* transgene appeared to shift the differentiation of thymocytes toward the CD8 lineage even in the context of class I deficiency. Thus, overexpressed Runx3 can push a cell toward the CD8 lineage independently of the MHC-elicited TCR signaling.

Overexpression of Runx3 can drive thymocytes toward the CD8 lineage irrespective of the CD4 signaling

In thymocyte differentiation, the TCR signaling exerts its effect in concert with the signaling elicited from either the CD4 or CD8 molecule. We examined the activity of overexpressed Runx3 on thymocyte differentiation under the condition of either excess or deficiency of CD4 signaling. First, the *Runx3*-transgene was introduced into human *CD4*-transgenic mice (Fig. 8*A*). As seen, the level of human CD4 expression was not so high and therefore might be limited to compensate the endogenous, murine CD4, which should be silenced by the overexpressed Runx3. Under this limitation, a majority of mature TCR^{high} cells possessed a $CD4^{-}8^{+}$ phenotype in *Runx3*-transgenic thymi. Second, the *Runx3*-transgene was expressed in a *CD4*-deficient background (Fig. 8*B*). When a $CD4^{-}8^{+}$ fraction was displayed for its TCR expression, the mature TCR^{high} cells corresponded to 27% of *CD4*-deficient and *Runx3*-transgenic thymocytes. In contrast, such mature cells occupied only 17% of simple *CD4*-deficient thymocytes. Collectively, neither an excess nor a lack of CD4 signaling appears to influence the extent of overproduction of mature $CD4^{-}8^{+}$ thymocytes, which is caused by the overexpressed Runx3. Thus, the activity of Runx3 to drive thymocytes toward the CD8 lineage is likely to be due to more than a simple silencing of *CD4* gene expression.

Discussion

Whether DP thymocytes select the CD8 or CD4 lineage is determined by the strength and/or duration of the TCR signal the cells receive through their interactions with an MHC/peptide complex (7, 22, 23). The DP cells cease expressing either the *CD4* or *CD8* gene, and thus eventually become committed to the CD8 SP or CD4 SP lineage, respectively. A *CD4* silencer element and the Runx binding sites in it play a pivotal role in the cessation of *CD4* expression (13, 24). Based on the analysis of thymocytes lacking *Runx1* or *Runx3*, Taniuchi et al. (13) proposed that Runx1 functions as an active repressor of *CD4* expression at the DN stage, whereas Runx3 is involved in the epigenetic silencing of the gene at the CD8 SP stage.

In the present study, we created *Runx3*-transgenic mice and found that the number of mature $CD4^{-}8^{+}$ thymocytes was increased. This result is opposite to that found in the *Runx3* (−/−) thymus, in which the number of mature $CD4^{-}8^{+}$ cells is markedly

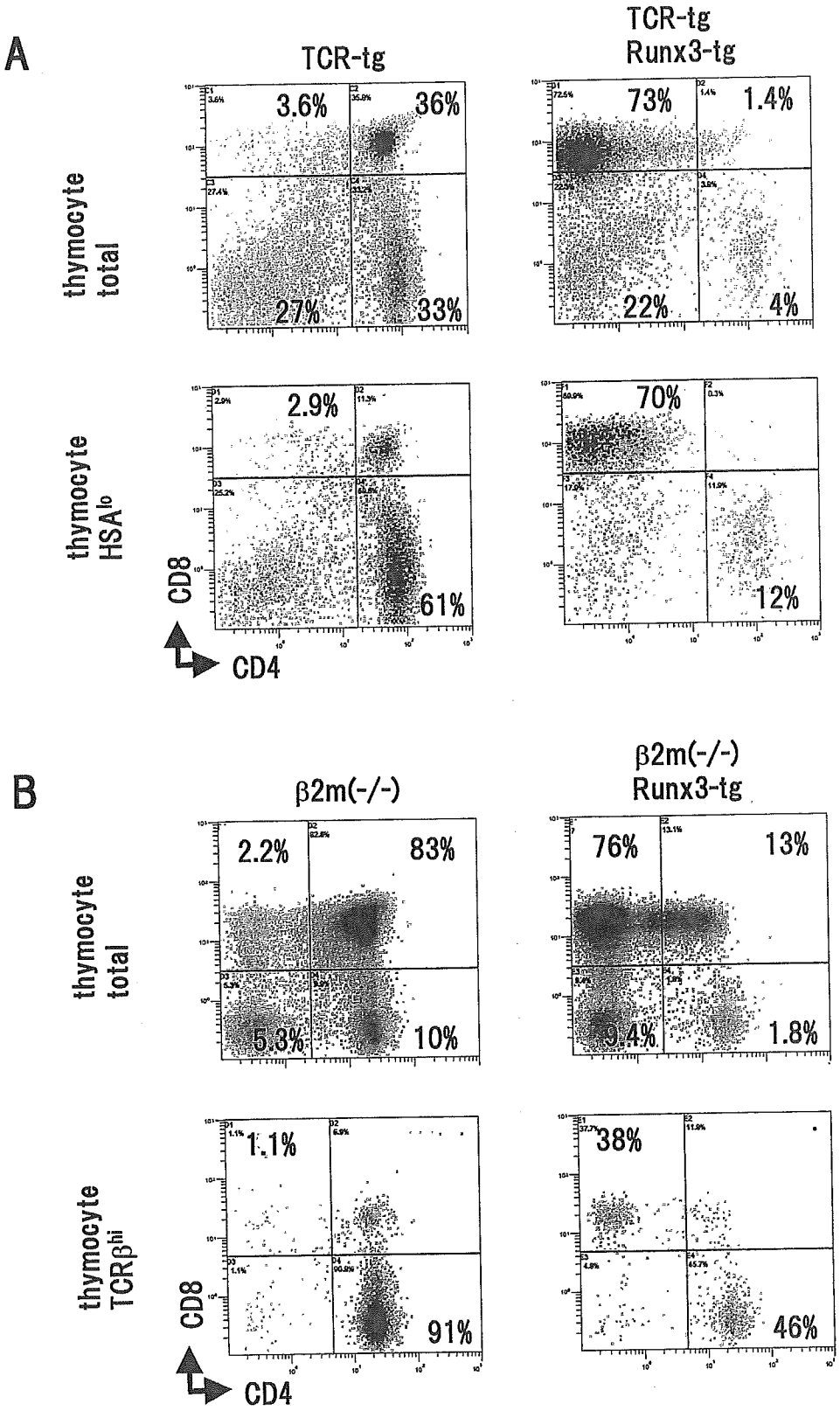

FIGURE 7. Effect of Runx3 overexpression on the differentiation potential of CD4-oriented thymocytes. *A*, The *TCR* transgene restricted to class II (*left*) was introduced into *Runx3*-transgenic mice (*right*). The CD4/CD8 expression profiles are shown for the nongated thymocytes (*upper panels*) as well as the mature, HSA^{low} thymocytes (*lower panels*). *B*, MHC class I deficiency (*left*) and the same deficiency coupled with the *Runx3*-transgene (*right*). The CD4/CD8 expression profiles are shown for the nongated thymocytes (*upper panels*) as well as the mature, TCR^{high} thymocytes (*lower panels*). The numbers in individual quadrants represent the percentages of cells of each type.

decreased (13, 14). Therefore, the present gain-of-function analysis complements the previous loss-of-function analysis. However, a close inspection of our results reveals a new aspect of Runx3 function as described below and as summarized in Fig. 9.

In the *Runx3*-transgenic thymus, the absolute number of mature $CD4^-8^+$ thymocytes was increased 2-fold compared with the nontransgenic thymus. This phenomenon cannot be explained solely by the effect of Runx3 on the *CD4* silencer. If *CD4* silencing had been overwhelming in the *Runx3*-transgenic mice, then the mature $CD4^+8^-$ thymocytes might also lose *CD4* expression, and a significant number of $CD4^-8^-TCR^{high}$ thymocytes might have been generated. However, we did not see evidence of such a population in the transgenic thymus. Mice lacking the *CD4* gene itself lose *CD4* expression completely, and the number of mature $CD4^-8^+$

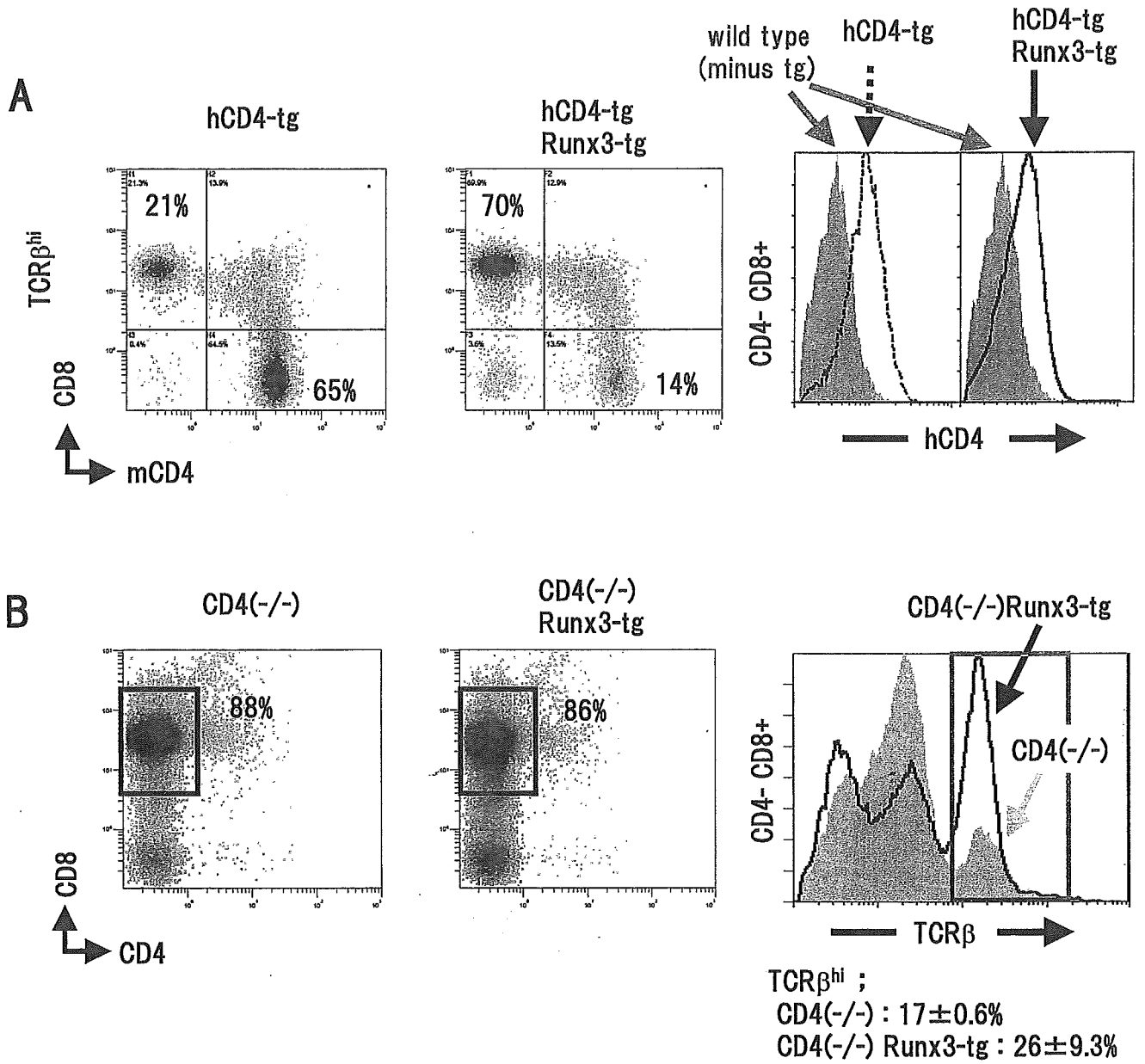

FIGURE 8. Effects of human *CD4* transgene and/or endogenous murine *CD4* deficiency on the differentiation of *Runx3*-transgenic thymocytes. *A*, The human *CD4* transgene driven by the murine *CD4* enhancer/promoter (*left*) was introduced into *Runx3*-transgenic mice (*middle*). The murine CD4/CD8 expression profiles are shown for the mature, TCR^{high} thymocytes (*left* and *middle*). In the *right panel*, the expression profiles of human CD4 are displayed for the murine $CD4^-8^+$ thymocytes. The shaded peak represents the wild-type cells, whereas the open peak represents the human *CD4*-single- and the human *CD4*- and *Runx3*-double-transgenic cells, respectively. *B*, A murine *CD4* deficiency (*left*) and the same deficiency coupled with the *Runx3*-transgene (*middle*). The CD4/CD8 expression profiles are shown for the nongated thymocytes (*left* and *middle*). In the *right panel*, the expression profiles of TCR are displayed for the gated $CD4^-8^+$ fraction. The shaded peak represents *CD4* (−/−) mice, whereas the open peak represents *CD4* (−/−):*Runx3*-transgenic mice.

thymocytes does not vary from that of wild-type mice (25). In contrast, we observed that overexpression of Runx3 could more efficiently convert the *CD4* (−/−) thymocytes to the mature $CD8^+$ cells. A similar result was obtained for the *Runx3*- and class II-restricted *TCR* double-transgenic mice as well as *Runx3*-transgenic:β_2m (−/−) mice. Taken together, Runx3 likely possesses the capacity not only to suppress *CD4* gene expression but also to actively drive the thymocytes toward the CD8 lineage.

In the wild-type thymus, the endogenous Runx3 is likely involved in the selection of and commitment to the CD8 lineage in concert with TCR signaling. A short and/or weak TCR signal is somehow transduced to Runx3, which in turn regulates the gene expression necessary for the CD8 lineage determination. *CD4* silencing is one target of Runx3 (13) and maintenance of *CD8* expression is probably a target as well. Another possibility is that Runx3 is involved in the survival and/or maturation of thymocytes after they have selected the CD8 lineage.

At the DN stage, the *CD4* silencer is reported to be "ON." Transcription of the *CD4* gene is initiated when the DN cells move to the DP stage, and the activity of the *CD4* silencer is expected to be turned "OFF" during the transition from DN to DP (26). The mechanism of this "OFF" switch cannot be assessed by targeted deletions of *Runx3* or *CD4* silencer. In our *Runx3*-transgenic thymus, the percentage and number of $CD4^+8^+$ cells were

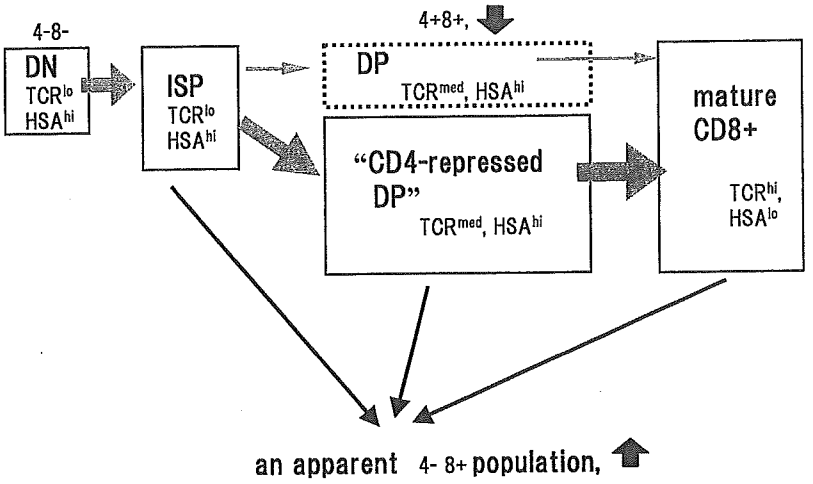

FIGURE 9. A model of T lymphocyte differentiation in the *Runx3*-transgenic thymus. Each step of differentiation is characterized by the specific expression patterns of CD4, CD8, TCR, and HSA. The cells usually start at the DN stage, go through the ISP and DP stages, and mature at the CD8 SP stage. The "CD4-repressed DP" stage is characterized by TCR^{med} expression; is apparently categorized as a $CD4^-8^+$ fraction; and is observed only in the *Runx3*-transgenic, but not the wild-type, thymus. The majority of mature $TCR^{high}HSA^{low}CD4^-8^+$ cells are considered to be derived from the premature "CD4-repressed DP" cells. A minor pathway for $CD8^+$ maturation in the transgenic animals would be through the usual "DP" stage.

remarkably reduced, and an aberrant population of "CD4-repressed DP" cells with a $CD4^-8^+TCR^{med}HSA^{high}$ phenotype emerged instead. It is likely that exogenous expression of the transgene-derived Runx3 protein maintained the *CD4* silencer in the "ON" position, thereby giving rise to the "CD4-repressed DP" thymocytes from the immature $CD4^-8^+TCR^{low}$ cells. However, these premature cells do acquire a $CD4^-8^+$ phenotype, probably due to the strong repression of *CD4* expression.

We previously reported the phenotype of *Runx1*-transgenic mice in which the numbers of both immature ISP and mature CD8 SP cells were increased (9). Even taking into consideration the differences between the *Runx3*- and *Runx1*-transgenic thymocytes in terms of the promoters used and/or the magnitude of transduced protein expression, it is interesting to note that overexpression of Runx1 did not generate the "CD4-repressed DP" cells as Runx3 did. Furthermore, the endogenous Runx1 protein is easily detected in the DP cells of wild-type thymus (10, 11), and Runx1 and Runx3 do not associate with each other in a coimmunoprecipitation experiment (K. Kohu and M. Satake, unpublished data). These observations suggest both that Runx1 is not involved in the turning the *CD4* silencer "OFF" at the DP stage and that the overexpressed Runx3 can reactivate the *CD4* silencer at this DP stage. It must be noted, though, that the enforced expression of Runx1 in a fetal thymic organ culture could generate similar "CD4-repressed DP" cells (27). The mechanism by which the *CD4* silencer is turned "OFF" at the DN-to-DP transition needs further investigation.

The *Runx3*-transgenic thymus clearly contained mature $CD4^+8^-$ cells, and we confirmed that the transduced Runx3 was indeed expressed in these cells. Perhaps in thymocytes that are committed to the $CD4^+8^-$ lineage, the chromatin structure at the *CD4* silencer region may be in a "closed" state, denying Runx3 access to the site.

Several transcription factors have been reported to be involved in the lineage selection of CD4/8 thymocytes. GATA3 is a positive regulator that boosts thymocytes toward the CD4 lineage (28–30), whereas TOX (31, 32) and/or activated Notch1 (33) move thymocytes toward the CD8 lineage. These factors are thought to function in response to an adequate signal from TCR when expressed endogenously, but transgenic overexpression might reveal cell-autonomous aspects of their functions. Thus, the possible interplay between the TCR signal, TOX, and Runx3 in the CD8 lineage selection will be a fascinating subject to pursue.

Acknowledgments

We are grateful to the following scientists for providing us with the valuable experimental tools: Y. Groner and D. Levanon for the murine *Runx3* cDNA, and R. Perlmutter for the proximal *Lck*-promoter. We express our thanks to M. Kuji for her secretarial assistance.

Disclosures

The authors have no financial conflict of interest.

References

1. Anderson, G., B. C. Harman, K. J. Hare, and E. J. Jenkinson. 2000. Microenvironmental regulation of T cell development in the thymus. *Semin. Immunol. 12:457.*
2. Varas, A., A. L. Hager-Theodorides, R. Sacedon, A. Vicente, A. G. Zapata, and T. Crompton. 2003. The role of morphogens in T-cell development. *Trends Immunol. 24:197.*
3. Basson, M. A., and R. Zamoyska. 2000. The CD4/CD8 lineage decision: integration of signalling pathways. *Immunol. Today 21:509.*
4. Germain, R. N. 2002. T-cell development and the CD4-CD8 lineage decision. *Nat. Rev. Immunol. 2:309.*
5. Alberola-Ila, J., and G. Hernandez-Hoyos. 2003. The Ras/MAPK cascade and the control of positive selection. *Immunol. Rev. 191:79.*
6. Rothenberg, E. V. 2002. T-lineage specification and commitment: a gene regulation perspective. *Semin. Immunol. 14:431.*
7. Singer, A. 2002. New perspectives on a developmental dilemma: the kinetic signaling model and the importance of signal duration for the CD4/CD8 lineage decision. *Curr. Opin. Immunol. 14:207.*
8. Hayashi, K., W. Natsume, T. Watanabe, N. Abe, N. Iwai, H. Okada, Y. Ito, M. Asano, Y. Iwakura, S. Habu, et al. 2000. Diminution of the AML1 transcription factor function causes differential effects on the fates of CD4 and CD8 single-positive T cells. *J. Immunol. 165:6816.*
9. Hayashi, K., N. Abe, T. Watanabe, M. Obinata, M. Ito, T. Sato, S. Habu, and M. Satake. 2001. Overexpression of AML1 transcription factor drives thymocytes into the CD8 single-positive lineage. *J. Immunol. 167:4957.*
10. Ehlers, M., K. Laule-Kilian, M. Petter, C. J. Aldrian, B. Grueter, A. Wurch, N. Yoshida, T. Watanabe, M. Satake, and V. Steimle. 2003. Morpholino antisense oligonucleotide-mediated gene knockdown during thymocyte development reveals role for Runx3 transcription factor in CD4 silencing during development of $CD4^-/CD8^+$ thymocytes. *J. Immunol. 171:3594.*
11. Sato, T., R. Ito, S. Nunomura, S. Ohno, K. Hayashi, M. Satake, and S. Habu. 2003. Requirement of transcription factor AML1 in proliferation of developing thymocytes. *Immunol. Lett. 89:39.*
12. Ichikawa, M., T. Asai, T. Saito, G. Yamamoto, S. Seo, I. Yamazaki, T. Yamagata, K. Mitani, S. Chiba, H. Hirai, et al. 2004. AML-1 is required for megakaryocytic maturation and lymphocytic differentiation, but not for maintenance of hematopoietic stem cells in adult hematopoiesis. *Nat. Med. 10:229.*
13. Taniuchi, I., M. Osato, T. Egawa, M. J. Sunshine, S. C. Bae, T. Komori, Y. Ito, and D. R. Littman. 2002. Differential requirements for Runx proteins in CD4 repression and epigenetic silencing during T lymphocyte development. *Cell 111:621.*
14. Woolf, E., C. Xiao, O. Fainaru, J. Lotem, D. Rosen, V. Negreanu, Y. Bernstein, D. Goldenberg, O. Brenner, G. Berke, et al. 2003. Runx3 and Runx1 are required for CD8 T cell development during thymopoiesis. *Proc. Natl. Acad. Sci. USA 100:7731.*
15. Levanon, D., V. Negreanu, Y. Bernstein, I. Bar-Am, L. Avivi, and Y. Groner. 1994. AML1, AML2, and AML3, the human members of the runt domain gene-family: cDNA structure, expression, and chromosomal localization. *Genomics 23:425.*
16. Garvin, A. M., K. M. Abraham, K. A. Forbush, A. G. Farr, B. L. Davison, and R. M. Perlmutter. 1990. Disruption of thymocyte development and lymphomagenesis induced by SV40 T-antigen. *Int. Immunol. 2:173.*
17. Sato, T., T. Sasahara, Y. Nakamura, T. Osaki, T. Hasegawa, T. Tadakuma, Y. Arata, Y. Kumagai, M. Katsuki, and S. Habu. 1994. Naive T cells can mediate

delayed-type hypersensitivity response in T cell receptor transgenic mice. *Eur. J. Immunol. 24:1512.*
18. Chiba, N., T. Watanabe, S. Nomura, Y. Tanaka, M. Minowa, M. Niki, R. Kanamaru, and M. Satake. 1997. Differentiation dependent expression and distinct subcellular localization of the protooncogene product, PEBP2β/CBFβ, in muscle development. *Oncogene 14:2543.*
19. Kanto, S., N. Chiba, Y. Tanaka, S. Fujita, M. Endo, N. Kamada, K. Yoshikawa, A. Fukuzaki, S. Orikasa, T. Watanabe, and M. Satake. 2000. The PEBP2β/CBFβ-SMMHC chimeric protein is localized both in the cell membrane and nuclear subfractions of leukemic cells carrying chromosomal inversion 16. *Leukemia 14:1253.*
20. Tanaka, Y., T. Watanabe, N. Chiba, M. Niki, Y. Kuroiwa, T. Nishihira, S. Satomi, Y. Ito, and M. Satake. 1997. The protooncogene product, PEBP2β/CBFβ, is mainly located in the cytoplasm and has an affinity with cytoskeletal structures. *Oncogene 15:677.*
21. Liu, X., and R. Bosselut. 2004. Duration of TCR signaling controls CD4-CD8 lineage differentiation in vivo. *Nat. Immunol. 5:280.*
22. Yasutomo, K., C. Doyle, L. Miele, C. Fuchs, and R. N. Germain. 2000. The duration of antigen receptor signalling determines $CD4^+$ versus $CD8^+$ T-cell lineage fate. *Nature 404:506.*
23. Hogquist, K. A. 2001. Signal strength in thymic selection and lineage commitment. *Curr. Opin. Immunol. 13:225.*
24. Zou, Y. R., M. J. Sunshine, I. Taniuchi, F. Hatam, N. Killeen, and D. R. Littman. 2001. Epigenetic silencing of CD4 in T cells committed to the cytotoxic lineage. *Nat. Genet. 29:332.*
25. Rahemtulla, A., W. P. Fung-Leung, M. W. Schilham, T. M. Kundig, S. R. Sambhara, A. Narendran, A. Arabian, A. Wakeham, C. J. Paige, R. M. Zinkernagel, et al. 1991. Normal development and function of $CD8^+$ cells but markedly decreased helper cell activity in mice lacking CD4. *Nature 353:180.*
26. Sawada, S., J. D. Scarborough, N. Killeen, and D. R. Littman. 1994. A lineage-specific transcriptional silencer regulates *CD4* gene expression during T lymphocyte development. *Cell 77:917.*
27. Telfer, J. C., E. E. Hedblom, M. K. Anderson, M. N. Laurent, and E. V. Rothenberg. 2004. Localization of the domains in Runx transcription factors required for the repression of CD4 in thymocytes. *J. Immunol. 172:4359.*
28. Nawijn, M. C., R. Ferreira, G. M. Dingjan, O. Kahre, D. Drabek, A. Karis, F. Grosveld, and R. W. Hendriks. 2001. Enforced expression of GATA-3 during T cell development inhibits maturation of CD8 single-positive cells and induces thymic lymphoma in transgenic mice. *J. Immunol. 167:715.*
29. Hernandez-Hoyos, G., M. K. Anderson, C. Wang, E. V. Rothenberg, and J. Alberola-Ila. 2003. GATA-3 expression is controlled by TCR signals and regulates CD4/CD8 differentiation. *Immunity 19:83.*
30. Pai, S. Y., M. L. Truitt, C. N. Ting, J. M. Leiden, L. H. Glimcher, and I. C. Ho. 2003. Critical roles for transcription factor GATA-3 in thymocyte development. *Immunity 19:863.*
31. Wilkinson, B., J. Y. Chen, P. Han, K. M. Rufner, O. D. Goularte, and J. Kaye. 2002. TOX: an HMG box protein implicated in the regulation of thymocyte selection. *Nat. Immunol. 3:272.*
32. Aliahmad, P., E. O'Flaherty, P. Han, O. D. Goularte, B. Wilkinson, M. Satake, J. D. Molkentin, and J. Kaye. 2004. TOX provides a link between calcineurin activation and CD8 lineage commitment. *J. Exp. Med. 199:1089.*
33. Robey, E., D. Chang, A. Itano, D. Cado, H. Alexander, D. Lans, G. Weinmaster, and P. Salmon. 1996. An activated form of Notch influences the choice between CD4 and CD8 T cell lineages. *Cell 87:483.*

THE JOURNAL OF BIOLOGICAL CHEMISTRY
Vol. 280, No. 8, Issue of February 25, pp. 7002–7009, 2005
Printed in U.S.A.

Deficiency of Interleukin-1 Receptor Antagonist Deteriorates Fatty Liver and Cholesterol Metabolism in Hypercholesterolemic Mice*

Received for publication, October 28, 2004, and in revised form, November 30, 2004
Published, JBC Papers in Press, December 1, 2004, DOI 10.1074/jbc.M412220200

Kikuo Isoda‡§¶, Shojiro Sawada‡§, Makoto Ayaori‡, Taizo Matsuki‖, Reiko Horai‖, Yutaka Kagata, Koji Miyazaki‡, Masatoshi Kusuhara‡, Mitsuyo Okazaki‡‡, Osamu Matsubara**, Yoichiro Iwakura‖, and Fumitaka Ohsuzu‡**

*From ‡Internal Medicine I and the **Second Department of Pathology, National Defense Medical College, Tokorozawa 359-8513, the ‖Center for Experimental Medicine, Institute of Medical Science, University of Tokyo, Tokyo 108-8639, and the ‡‡Laboratory of Chemistry, College of Liberal Arts and Sciences, Tokyo Medical and Dental University, Chiba 272-0827, Japan*

Although the anti-inflammatory effect of interleukin-1 (IL-1) receptor antagonist (IL-1Ra) has been described, the contribution of this cytokine to cholesterol metabolism remains unclear. Our aim was to ascertain whether deficiency of IL-1Ra deteriorates cholesterol metabolism upon consumption of an atherogenic diet. IL-1Ra-deficient mice (IL-1Ra$^{-/-}$) showed severe fatty liver and portal fibrosis containing many inflammatory cells following 20 weeks of an atherogenic diet when compared with wild type (WT) mice. Expectedly, the levels of total cholesterol in IL-1Ra$^{-/-}$ mice were significantly increased, and the start of lipid accumulation in liver was observed earlier when compared with WT mice. Real-time PCR analysis revealed that IL-1Ra$^{-/-}$ mice failed to induce mRNA expression of cholesterol 7α-hydroxylase, which is the rate-limiting enzyme in bile acid synthesis, with concurrent up-regulation of small heterodimer partner 1 mRNA expression. Indeed, IL-1Ra$^{-/-}$ mice showed markedly decreased bile acid excretion, which is elevated in WT mice to maintain cholesterol level under atherogenic diet feeding. Therefore, we conclude that the lack of IL-1Ra deteriorates cholesterol homeostasis under atherogenic diet-induced inflammation.

When compared with other organs, the liver has one of the largest populations of macrophages, which are key components of the innate immune system. Resident hepatic macrophages, *i.e.* Kupffer cells, are derived from circulating monocytes that arise from bone marrow progenitors. Once localized within the liver, these cells differentiate to perform specialized functions, including phagocytosis. Kupffer cells also generate various products, including cytokines. These factors regulate not only the phenotypes of the Kupffer cells that produce them but also the phenotypes of neighboring cells, such as hepatocytes (1). Many recent studies suggest that several proinflammatory cytokines produced by activated Kupffer cells might be involved in the onset of liver disease, including alcoholic and nonalcoholic fatty liver disease (NAFLD)[1] (2–4). For instance, elevated circulating levels of tumor necrosis factor-α, IL-1β, and IL-6 have been observed in human patients (5) and animal models of both NAFLD (4) and alcohol-induced liver injury (6).

In contrast to proinflammatory cytokines, anti-inflammatory cytokines are considered to have hepato-protective effects (5). IL-1 receptor antagonist (IL-1Ra) is one of the negative regulators to IL-1 signaling by binding and blocking the functional receptor (IL-1 receptor type-I) without activation (7). IL-1Ra plays an anti-inflammatory role in acute and chronic inflammation (8). IL-1Ra is also produced by hepatocytes as well as macrophages/monocytes as an acute phase protein *in vivo* (9). Furthermore, we recently reported that IL-1Ra-deficient (IL-1Ra$^{-/-}$) mice showed decreased weight gain when consuming the same amount of food as wild-type mice and that body lipid accumulation remained impaired even when they were fed a high fat diet (10). However, the function of IL-1Ra in NAFLD is still not yet well understood.

Atherogenic diet has been widely used to study atherogenesis in animal models. Early atherogenic diets contained high concentrations of cholesterol (5%) and fat (30%) either supplemented with cholic acid (2%) (11) or fed in combination with irradiation treatments (12). These early diets produced high mortality and were subsequently modified to reduce the concentrations of cholesterol (1.25%), fat (15%), and cholate (0.5%) (13). Although this modified atherogenic diet produces an atherogenic lipoprotein profile and fatty streak lesions (14), it also induces inflammatory gene expression in the liver (15). Furthermore, it has been reported that a fat-enriched diet induced NAFLD in animal models (4).

It is now well recognized that inflammation or cytokines increase serum lipid levels (16, 17). This increase in serum lipid levels can be considered part of the acute phase response that results in marked changes in the levels of a large number of circulating protein primarily due to alterations in the liver (18). However, the role of IL-1Ra on lipid metabolism remains poorly understood.

To address the question more directly whether deficiency of IL-1Ra promotes development of NAFLD and changes lipid metabolism, we employed IL-1Ra$^{-/-}$ mice we had recently gen-

* This work was supported by a grant from the National Defense Medical College, Tokorozawa, Japan. The costs of publication of this article were defrayed in part by the payment of page charges. This article must therefore be hereby marked "*advertisement*" in accordance with 18 U.S.C. Section 1734 solely to indicate this fact.

§ Both authors contributed equally to this work.
¶ To whom correspondence should be addressed: Internal Medicine I, National Defense Medical College, 3-2, Namiki, Tokorozawa, Saitama, 359-8513, Japan. Tel.: 81-42-995-1597; Fax: 81-42-996-5200; E-mail: isoda@me.ndmc.ac.jp.

[1] The abbreviations used are: NAFLD, nonalcoholic fatty liver disease; ACAT2, Acyl-CoA cholesterol acyltransferase 2; ALT, alanine aminotransferase; Ct, threshold cycle number; CYP7A1, cholesterol 7α-hydroxylase; CYP27A1, sterol 27-hydroxylase; IL-1, interleukin-1; IL-1Ra, IL-1 receptor antagonist; IL-1Ra$^{-/-}$, IL-1Ra-deficient; LRH-1, liver receptor homolog-1; SHP, small heterodimer partner 1; SR-BI, scavenger receptor class B type I; WT, wild type; HPLC, high pressure liquid chromatography; LDL, low density lipoprotein; HDL, high density lipoprotein; VLDL, very low density lipoprotein; HMG, human menopausal gonadotropin; JNK, c-Jun N-terminal kinase.

TABLE I
PCR primers

LXRα, nuclear liver X-receptor α; FXR, farnesoid X-receptor (FXR); TGF, transforming growth factor.

	Forward	Reverse
ACAT2	5′-GCCCCAGATTCTACAAGCAAGA-3′	5′-TGTGGTAGATGGTTCGGAAATG-3′
HMG-CoA reductase	5′-TTTCTAGAGCGAGTGCATTAGCA-3′	5′-GATTGCCATTCCACGAGCTATAT-3′
18S rRNA	5′-AGTCGGAGGTTCGAAGACGAT-3′	5′-GCGGGTCATGGGAATAACG-3′
CYP7A1	5′-GCTGAGAGCTTGAAGCACAAGA-3′	5′-TTGAGATGCCCAGAGGATCAC-3′
LXRα	5′-GAGTTCTCCAGAGCCATGAATGA-3′	5′-CATATGTGTGTTGCAGCCTCTCTA-3′
SREBP2	5′-GTTCTGAGGAAGGCCATTGATT-3′	5′-CCACATCACTGTCCACCAGACT-3′
LDL receptor	5′-CCAGTGTGACCGTGAACATGA-3′	5′-TCCCCACTGTGACACTTGAACT-3′
SHP	5′-AGCTGGGTCCCAAGGAGTATG-3′	5′-ACCAGGGCTCCAAGACTTCA-3′
FXR	5′-ATCTCCGCCGAACGAAGAA-3′	5′-GGACCACGAAGATCAGATTGC-3′
CYP27A1	5′-GCCTTGCACAAGGAAGTGACT-3′	5′-CGCAGGGTCTCCTTAATCACA-3′
LRH-1	5′-ACTGAGAAATTCGGACAGCTACTTC-3′	5′-AGGTAGTCTTCTGCCTGCTTGCT-3′
ABCA1	5′-CCCAGAGCAAAAAGCGACTC-3′	5′-GGTCATCATCACTTTGGTCCTTG-3′
SR-B1	5′-TTCAGGGCGTCCAGAA-3′	5′-GATCTTGCTGAGTCCGTTCCA-3′
IL-1Ra	5′-CTTTACCTTCATCCGCTCTGAGA-3′	5′-TCTAGTGTTGTGCAGAGGAACCA-3′
IL-1 β	5′-TGGTGTGTGACGTTCCCATT-3′	5′-CAGCACGAGGCTTTTTTGTTG-3′
CD68	5′-ATAGCCCAAGGAACAGAGGAAGA-3′	5′-GGATGTAGGTGTCATCGTGAAG-3′
TGF β	5′-ACAAGGCTGCCCCGACTAC-3′	5′-GTTGACTTTCTCCTGGTATGAGATAGC-3′

erated (19). The present study aimed to definitively test the hypothesis that deficiency of IL-1Ra promotes NAFLD and alters lipid metabolism employing IL-1Ra$^{-/-}$ and wild type (WT) mice on atherogenic diet.

EXPERIMENTAL PROCEDURES

Animals and Experimental Procedure—The creation of IL-1Ra$^{-/-}$ mice used in this study has been described previously (19). In these mutant mice, the genes for all four isoforms of the IL-1Ra were disrupted. These mice were backcrossed to C57BL/6J strain mice for eight generations. IL-1Ra genotyping was performed by a polymerase chain reaction analysis of tail DNA as described previously (19). We used only male mice to rule out gender differences. IL-1Ra$^{-/-}$ mice and corresponding WT mice, derived by intercrossing WT littermates for knock-out, were studied at different times. Mice were maintained on a 12-h light/12-h dark cycle and fed a normal rodent diet containing 4.6% crude fat with less than 0.02% cholesterol (Clea Japan, Inc., Tokyo, Japan). Eight-week-old mice were switched to a high fat/cholesterol and cholate diet containing 15% total fat (8% cocoa butter), 1.25% cholesterol, and 0.5% sodium cholate (Clea Japan), hereafter referred to as the atherogenic diet. IL-1Ra$^{-/-}$ and WT mice were characterized immediately before and after consumption of the atherogenic diet for 1, 4, 8, and 20 weeks. The studies were carried out according to the protocols approved by the National Defense Medical College Board for Studies in Experimental Animals.

Chemical Analysis of Serum and Tissue—On the day of analysis, food was removed from the cages in the morning, and the mice were fasted for 7 h. Blood was drawn from mice by cardiac puncture under light methoxyflurane anesthesia. Animals were sacrificed by cervical dislocation, and livers were immediately collected and weighed, and tissue samples were divided; some were fixed in 4% paraformaldehyde, and others were frozen in liquid nitrogen and stored at −80 °C. Blood was transferred into tubes, and serum was collected by centrifugation. Serum alanine aminotransferase (ALT) determination was performed using a commercially available assay kit according to the manufacturer's instructions (Sigma diagnostic kit; Sigma). Plasma analysis of albumin and bilirubin levels was performed using a Paramax RX automated analyzer (Dade International). The plasma total cholesterol, HDL cholesterol, and triglyceride levels were measured by enzymatic assays as described previously (20). Furthermore, plasma lipoproteins were analyzed by an on-line dual enzymatic method for simultaneous quantification of cholesterol and triglycerides by HPLC at Skylight Biotech Inc. (Akita, Japan) according to the procedure as described by Usui *et al.* (21). 200 μl of 20× saline-diluted sera was injected into two tandem connected TSK gel LipopropakXL columns (300 × 7.8-mm; Tosoh), and cholesterol and triglyceride contents in lipoproteins separated by size were determined by using enzymatic reagents specially prepared by Kyowa Medex (Tokyo, Japan). Total cholesterol and triglyceride concentrations (in mg/dL) were calculated by comparison with total area under the chromatographic curves of a calibration standard of known concentration (22). Hepatic lipids were extracted according to the methods of Folch *et al.* (23). The extract was dissolved in 2-propanol and subsequently analyzed for total cholesterol, free cholesterol, and triglycerides using a commercially available reagent (TC kit, FC kit, and TG kit, Wako, Japan).

Analysis of Fecal Bile Acids—Stools were collected from each animal over 72 h immediately prior to study, dried, weighed, and ground in a mechanical blender. Aliquots were taken for the measurement of total bile acid content by an enzymatic method as described (24). The daily stool output (g/day/100 g of body weight) and fecal bile acid content (μmol/g of stool) were used to calculate the rate of bile acid excretion (μmol/day/100 g of body weight).

Tissue Preparation and Histology—Livers were harvested, fixed overnight in 4% paraformaldehyde, embedded in OCT compounds (Tissue-Tek; Sakura Finetechnical Co., Tokyo, Japan), and sectioned (10-μm thickness). All samples were routinely stained with hematoxylin-eosin, Masson's trichrome, and oil red O.

Analysis of Gene Expression by Real-time Quantitative PCR—Total RNA was isolated from each mouse liver using Tri Reagent (Sigma) according to the manufacturer's instructions. Purified RNA was reverse-transcribed according to the protocols supplied by the manufacturer. Quantitative gene expression analysis was performed on an ABI PRISM 7700 machine (Applied Biosystems) using SYBR Green technology. PCR primers (Table I) were designed using Primer Express 1.7 software with the manufacturer's default settings (Applied Biosystems) and validated for identical efficiencies (slope = −3.3 for a plot of Ct *versus* a log of ng of cDNA). In 96-well optical plates, 12.5 μl of SYBR Green master mix was added to 12.5 μl of cDNA (corresponding to 50 ng of total RNA input) and 300 nM forward and reverse primers in water. Plates were heated for 2 min at 50 °C and 10 min at 95 °C. Subsequently, 40 PCR cycles consisting of 15 s at 95 °C and 60 s at 60 °C were applied. At the end of the run, samples were heated to 95 °C with a ramp time of 20 min to construct dissociation curves to check that single PCR products were obtained. The absence of genomic DNA contamination in the RNA preparations was confirmed by using total RNA samples that had not been reverse-transcribed. 18S was used as the standard housekeeping gene. The ratio of target gene and 18S expression levels (relative gene expression numbers) was calculated by subtracting the threshold cycle number (Ct) of the target gene from the Ct of *18S* and raising 2 to the power of this difference. Ct values are defined as the number of PCR cycles at which the fluorescent signal during the PCR reaches a fixed threshold. Target gene mRNA expression is thus expressed relative to 18S expression.

Statistical Analysis—The results are shown as the mean ± S.E. except the values of serum ALT, bilirubin, and albumin, which were determined using plasma pooled from groups of five mice. Two groups were compared using Student's t test or Student-Newman Keuls's test with the one-way analysis of variance. A value of $p < 0.05$ was regarded as a significant difference.

RESULTS

Liver Size and Serum Transaminase—Analysis of livers of IL-1Ra$^{-/-}$ mice fed a standard laboratory rodent chow indicated that these mice appeared identical to those of WT mice as determined by morphological and histological studies (data not shown). We next tested the effect of an atherogenic diet (chow supplemented with 15% fat, 1.25% cholesterol, and 0.5% sodium cholate). In contrast to little changes in WT mice, there

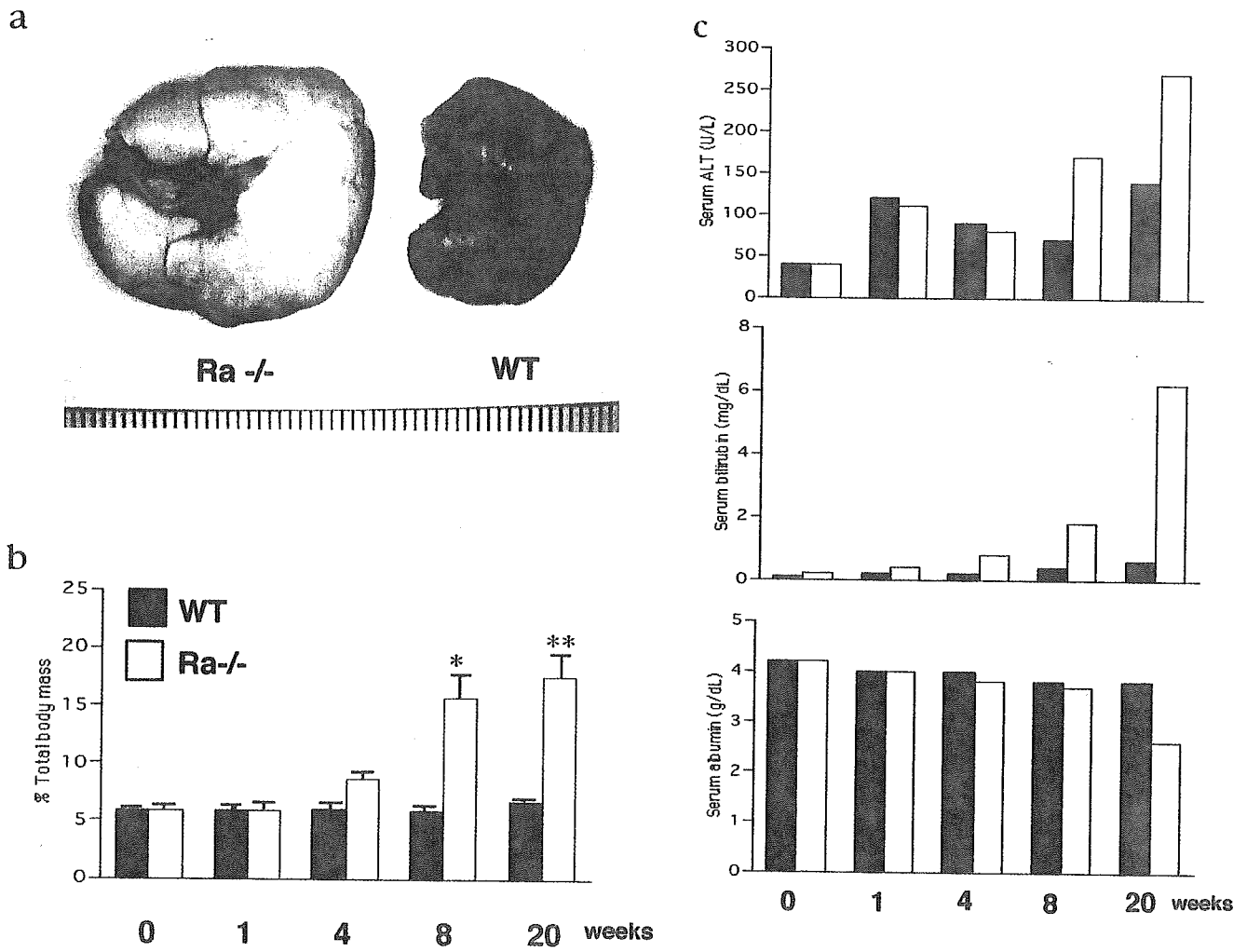

FIG. 1. **Effects of atherogenic diet on liver morphology, liver size, and serum ALT, bilirubin, and albumin.** *a*, macroscopic appearance of livers from IL-1Ra$^{-/-}$ (*Ra*$^{-/-}$) and WT mice fed an atherogenic diet for 20 weeks. *b*, liver mass relative to the total body mass of IL-1Ra$^{-/-}$ and WT mice fed an atherogenic diet for 0, 1, 4, 8, or 20 weeks. *, $p < 0.05$; **, $p < 0.01$ for IL-1Ra$^{-/-}$ mice *versus* WT mice. *c*, the *upper panel* shows the serum ALT levels of IL-1Ra$^{-/-}$ and WT mice fed chow supplemented with the atherogenic diet for 0, 1, 4, 8, or 20 weeks. The *middle panel* shows serum bilirubin level, and the *lower panel* shows serum albumin level. The measurements of all these markers were performed on plasma pooled from groups of five male mice.

were dramatic morphological changes in the livers of IL-1Ra$^{-/-}$ mice fed the same diet (Fig. 1). Following 20 weeks of atherogenic diet, there was a prominent color and size change in the livers of IL-1Ra$^{-/-}$ mice *versus* WT mice (Fig. 1*a*). Four weeks after the start of the atherogenic diet, the liver weight to body weight ratios in the IL-1Ra$^{-/-}$ mice tended to become larger (but not significant) than those of WT (8.6 ± 0.9%, $n = 5$ *versus* 6.0 ± 0.6%, $n = 5$; p = NS; Fig. 1*b*). Following 8 weeks of the atherogenic diet, this parameter increased by 166% in IL-1Ra$^{-/-}$ mice when compared with WT mice (15.7 ± 2.6%, $n = 5$ *versus* 5.9 ± 0.5%, $n = 5$; $p < 0.05$). Following 20 weeks of the atherogenic diet, the parameter increased ~3-fold when compared with before atherogenic diet feeding in IL-1Ra$^{-/-}$ mice; however, the atherogenic diet caused only a small increase in liver weight to body weight ratios in WT mice (17.6 ± 2.4%, $n = 5$ *versus* 6.7 ± 0.6%, $n = 5$; $p < 0.01$). In conclusion, continued atherogenic diet caused significantly greater enlargement of livers in IL-1Ra$^{-/-}$ mice than in WT mice.

As markers of liver injury, serum ALT, bilirubin, and albumin were monitored throughout the study. Before atherogenic diet, the serum level of ALT in both IL-1Ra$^{-/-}$ and WT mice was 40 units/liters. Following 20 weeks of atherogenic diet, the serum levels of ALT and bilirubin increased by 93 and 875%, respectively, in IL-1Ra$^{-/-}$ mice when compared with WT mice (Fig. 1*c*). In contrast, the serum level of albumin decreased by 28% when compared with WT mice (Fig. 1*c*). We detected moderate ascites in all IL-1Ra$^{-/-}$ mice but not in WT mice 20 weeks after the start of atherogenic diet. These data suggest that the atherogenic diet induces a more severe liver injury in IL-1Ra$^{-/-}$ mice than in WT mice.

Histopathological Changes—Histological examination of livers from both mice demonstrated a time-dependent increase of the number and size of intracellular vacuoles, characteristics of lipid deposits (Fig. 2). These changes, however, were prominent in IL-1Ra$^{-/-}$ but not WT livers. Furthermore, following 20 weeks of the atherogenic diet, the morphology of the IL-1Ra$^{-/-}$ livers had been substantially altered, including extensive portal fibrosis and collagen deposition in a pericellular distribution in the lobule (Fig. 2*b*). Moreover, both lobular and portal inflammation was detected in IL-1Ra$^{-/-}$ liver (Fig. 2*b*).

Oil red O staining of livers from both types of mice revealed that the deposition of neutral lipid increased in a time-dependent manner (Fig. 3). However, the start of lipid deposition in IL-1Ra$^{-/-}$ livers occurred earlier when compared with the WT livers. Indeed, we could detect lipid deposits in IL-1Ra$^{-/-}$ liver after 1 week of atherogenic diet, with no deposits in WT liver. Furthermore, as expected from the gross morphology, neutral

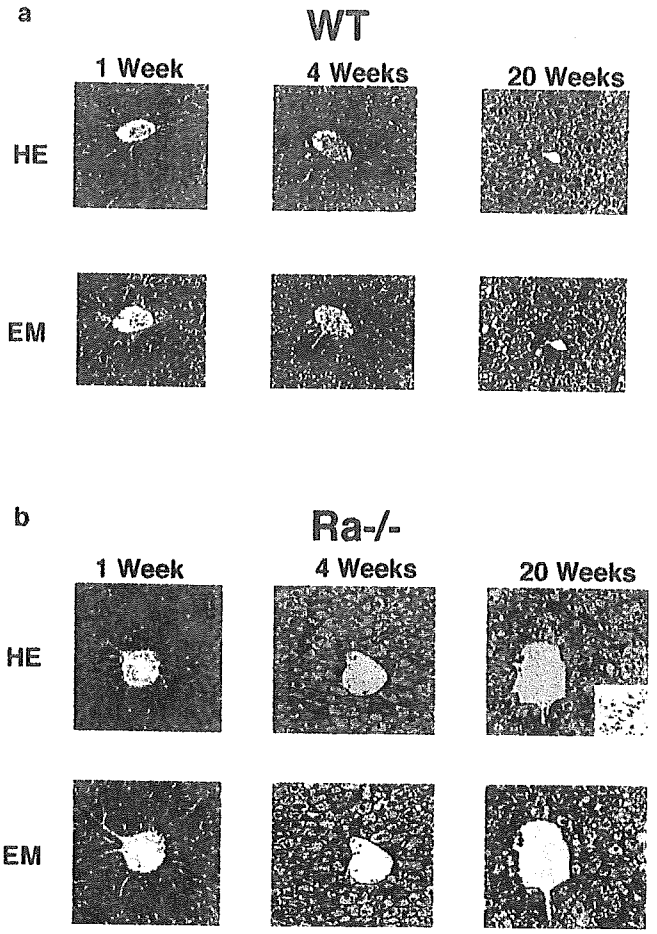

FIG. 2. **Effect of deficiency of IL-1Ra on atherogenic diet-induced steatosis and inflammation.** Liver specimens were taken from wild type (*a*) and IL-1Ra$^{-/-}$ (*b*) mice fed an atherogenic diet for 1, 4, or 20 weeks. Portal and lobular inflammation in IL-1Ra$^{-/-}$ liver was more prominent at 20 weeks of the atherogenic diet (*inset*, lobular inflammation). Liver sections were prepared for histology and stained with hematoxylin and eosin (*HE*) or Masson's trichrome (*EM*).

lipid accumulation was markedly more pronounced in the IL-1Ra$^{-/-}$ than the WT liver following 20 weeks of atherogenic diet.

Alteration of Lipid Homeostasis in IL-1Ra$^{-/-}$ Mice—Following 4 weeks of the atherogenic diet, levels of total plasma cholesterol did not differ between IL-1Ra$^{-/-}$ and WT mice (224.9 ± 12.4 mg/dl *versus* 207.1 ± 20.5 mg/dl; $n = 5$: p = NS; Fig. 4*a*). However, after 8 weeks of the atherogenic diet, the levels of total cholesterol in IL-1Ra$^{-/-}$ mice increased by 198% when compared with WT mice (610 ± 224 mg/dl, *versus* 205 ± 12 mg/dl; $n = 5$; $p < 0.05$). After 20 weeks of atherogenic diet, moreover, the total cholesterol levels increased significantly in IL-1Ra$^{-/-}$ mice when compared with WT mice (942 ± 160 mg/dl *versus* 240 ± 13 mg/dl, $n = 5$; $p < 0.01$).

High resolution HPLC analysis of plasma lipoproteins following 4 weeks of the atherogenic diet revealed no significant differences in the levels of chylomicron-, VLDL-, LDL-, and HDL-cholesterol between the IL-1Ra$^{-/-}$ and WT mice (Fig. 4, *b* and *c*). However, after 20 weeks of atherogenic diet, HPLC analysis revealed markedly increased cholesterol levels in the VLDL and LDL fractions in the IL-1Ra$^{-/-}$ mice when compared with the WT mice. The cholesterol levels in the VLDL and LDL fractions were 699 ± 126 mg/dl ($n = 5, p < 0.01$) and 192 ± 36 mg/dl ($n = 5$, $p < 0.01$), respectively in IL-1Ra$^{-/-}$ mice when compared with 136 ± 7 mg/dl ($n = 5$) and 50 ± 4 mg/dl ($n = 5$), respectively, in the WT mice. In contrast, levels

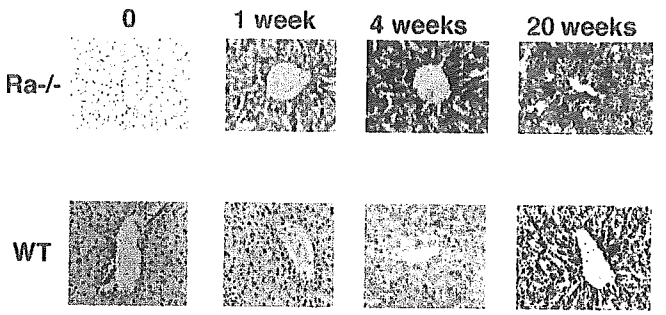

FIG. 3. **Effect of deficiency of IL-1Ra on atherogenic diet-induced lipid accumulation in the liver.** Liver specimens were taken from IL-1Ra$^{-/-}$ (*Ra$^{-/-}$*) and WT mice fed an atherogenic diet for 0, 1, 4, or 20 weeks. Liver sections were prepared for histology and stained with oil red O.

of HDL-cholesterol were significantly lower in IL-1Ra$^{-/-}$ mice (31 ± 10 mg/dl, $n = 5$) when compared with those in WT mice (54 ± 3 mg/dl, $n = 5$; $p < 0.05$; Fig. 4, *b* and *c*).

The hepatic cholesterol levels of both mice showed a time-dependent increase (Fig. 5). However, these changes were more prominent in the liver of IL-1Ra$^{-/-}$ than in WT mice, and the difference between these mice increased with prolonged diet. In agreement with the enlarged liver and distinct color change, hepatic cholesterol was significantly increased in IL-1Ra$^{-/-}$ mice after 20 weeks of the atherogenic diet regimen. No significant differences were observed for hepatic triglyceride levels between the IL-1Ra$^{-/-}$ and WT mice. The major component of hepatic cholesterol in both genotypes was cholesterol ester.

Alteration of Bile Acids and Cholesterol Metabolism in IL-1Ra$^{-/-}$ Mice—The primary route of cholesterol elimination from the body is via bile, which is based on conversion of hepatic cholesterol to bile acids. Fecal bile acid excretion of WT mice increased with the duration of atherogenic diet; however, in IL-1Ra$^{-/-}$ mice, bile acid excretion was increasingly impaired under continued atherogenic diet (Fig. 6).

Alteration of mRNA Expressions in IL-1Ra$^{-/-}$ Mice—Analyses of mRNA expression of genes involved in cytokine, monocyte activation, and the regulation of cholesterol, fatty acid, and bile acid metabolism were performed to identify pathways potentially responsible for the observed alterations in IL-1Ra$^{-/-}$ mice. Real-time PCR employed mRNA extracted from livers of both mice (Fig. 7). Prior to the start of the atherogenic diet (0 week), expression levels of cholesterol 7α-hydroxylase (CYP7A1) in IL-1Ra$^{-/-}$ mice were 30% lower than those in WT mice ($p < 0.05$; Fig. 7*a*). After 1 and 4 weeks of atherogenic diet, CYP7A1 expression decreased in both mice; however, transcript levels in IL-1Ra$^{-/-}$ mice were markedly lower (or absent). These results suggest that bile acid biosynthesis in IL-1Ra$^{-/-}$ mice might be attenuated as early as 1 week after the start of the atherogenic diet regimen. Although a previous study showed that lipopolysaccharide suppresses both CYP7A1 and sterol 27-hydroxylase (CYP27A1) (25), expression levels of CYP27A1 in both IL-1Ra$^{-/-}$ and WT mice decreased after 1 week of the atherogenic diet, and there was no significant difference between these two groups (Fig. 7*c*). Although atherogenic diet increased small heterodimer partner 1 (SHP) mRNA in both mice, expression was 1.8-fold higher ($p < 0.01$) after 1 week and 3-fold higher ($p < 0.001$) after 4 weeks of the atherogenic diet in IL-1Ra$^{-/-}$ when compared with WT mice (Fig. 7*b*). Furthermore, expression of liver receptor homolog-1 (LRH-1) increased in both mice after 4 weeks of atherogenic diet; however, a 1.8-fold higher ($p < 0.05$) increase was observed in IL-1Ra$^{-/-}$ mice when compared with WT mice (Fig. 7*c*). Moreover, after 1 week of the atherogenic diet, mRNA expression of Acyl-CoA cholesterol acyltransferase 2 (ACAT2) was only mar-

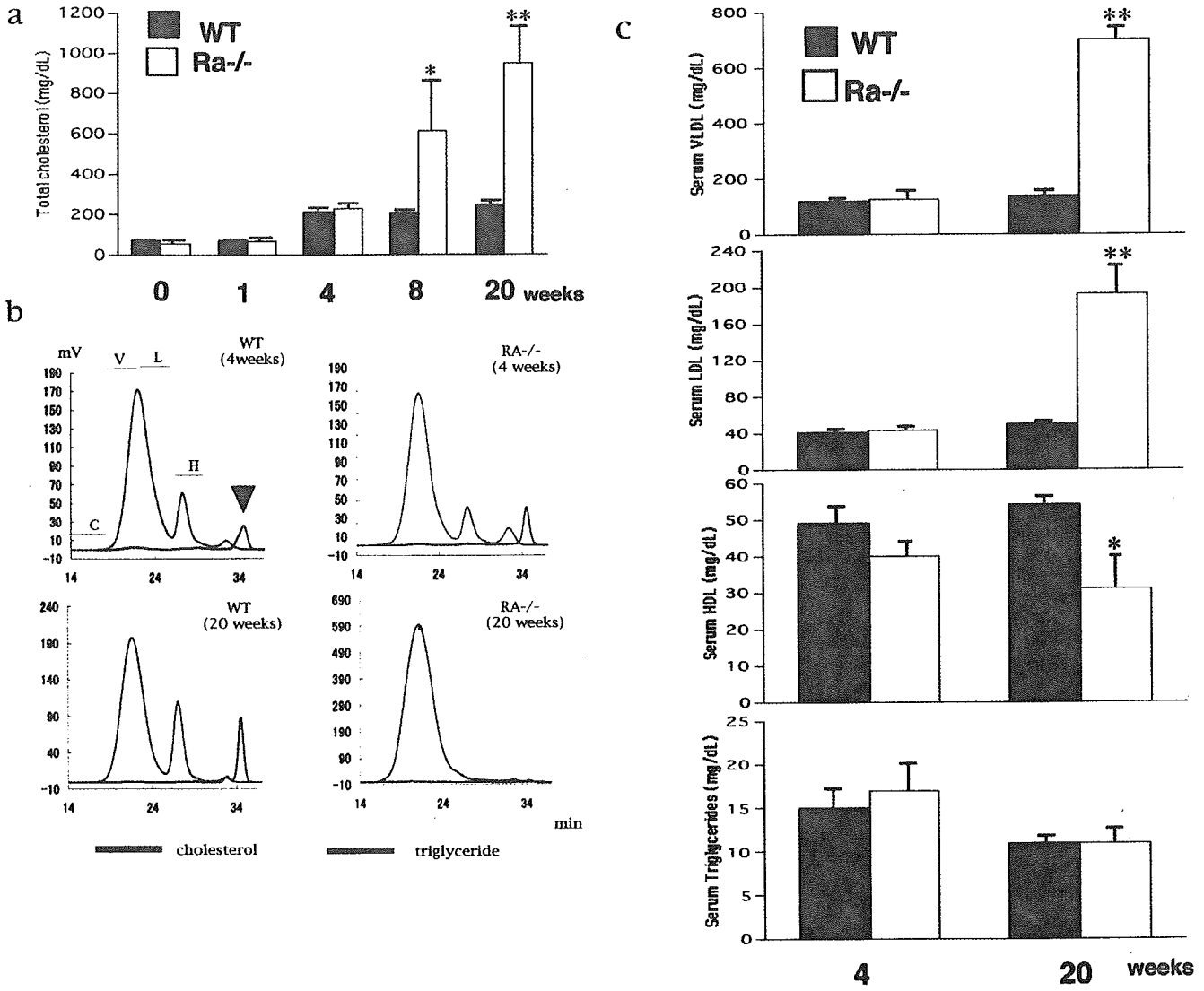

FIG. 4. **The duration of atherogenic diet-dependent changes in plasma cholesterol concentrations in mice with different genotypes.** *a*, plasma levels of total cholesterol of IL-1Ra$^{-/-}$ (*Ra*$^{-/-}$) and WT mice fed chow supplemented with the atherogenic diet for 0, 1, 4, 8, or 20 weeks. The levels of total cholesterol were determined enzymatically after 7 h of fasting. All values are expressed as mean ± S.E. *, $p < 0.05$; **, $p < 0.01$ for IL-1Ra$^{-/-}$ mice *versus* WT mice. *b*, HPLC analysis of plasma lipoproteins. Plasma samples from mice of each genotype following 4 and 20 weeks of the atherogenic diet were separated by HPLC, and cholesterol (*red line*) and triglyceride (*blue line*) contents were determined. The chylomicron, VLDL, LDL, and HDL fractions are labeled *C*, *V*, *L*, and *H*, respectively. Free glycerol is indicated by an *arrowhead*. *c*, plasma levels of VLDL (*upper*), LDL (*middle upper*), HDL (*middle lower*), and triglycerides (*lower*) of IL-1Ra$^{-/-}$ and WT mice. The levels of these lipids were calculated from HPLC results. All values are expressed as mean ± S.E. *, $p < 0.05$; **, $p < 0.01$ for IL-1Ra$^{-/-}$ mice *versus* WT mice.

ginally if at all increased in the IL-1Ra$^{-/-}$ mice, whereas a 2-fold increased level was observed after 4 weeks of the atherogenic diet ($p < 0.05$;Fig. 7*a*). In contrast, no differences were observed in hepatic expression of LDL receptor, HMG-CoA reductase, SREBP2, nuclear liver X-receptor α, and farnesoid X-receptor between IL-1Ra$^{-/-}$ and WT mice. Furthermore, hepatic expression of the HDL-cholesterol regulatory genes ATP binding cassette-A1 (*ABCA1*) and scavenger receptor class B type I (*SR-BI*) did not differ between IL-1Ra$^{-/-}$ and WT mice.

IL-1Ra, as expected, was absent in IL-1Ra$^{-/-}$ mice, whereas the expression level of IL-1β in IL-1Ra$^{-/-}$ mice was significantly elevated even before atherogenic diet ($p < 0.05$) and more than 10-fold ($p < 0.001$) up-regulated following 4 weeks of the atherogenic diet (Fig. 7*d*). Moreover, 4 weeks of atherogenic diet increased transforming growth factor-β (4.5-fold, $p < 0.01$) and CD68 (7-fold, $p < 0.01$) in the IL-1Ra$^{-/-}$ mice when compared with WT mice.

DISCUSSION

The present study demonstrates that IL-1Ra$^{-/-}$ mice develop severe NAFLD and portal fibrosis with many inflammatory cells following 20 weeks of the atherogenic diet when compared with WT mice. We also found that mRNA levels of IL-1β and transforming growth factor-β were significantly elevated in livers of IL-1Ra$^{-/-}$ mice. These findings are in accord with several previous studies implicating cytokine imbalances in murine models of NAFLD (4) and fibrosis (26, 27). These findings suggest that cytokines, such as IL-1β, may play an important role in the pathogenesis of NAFLD and hepatic fibrosis. In our IL-1Ra$^{-/-}$ mice, excessive IL-1 signaling may induce inflammation in the liver and, thus, the IL-1 system might play a role in the development of NAFLD and fibrosis. The atherogenic diet we used in this study appears associated with these dramatic changes in the livers of IL-1Ra$^{-/-}$ mice, corroborating a recent study showing that high cholesterol levels induce expression of several genes

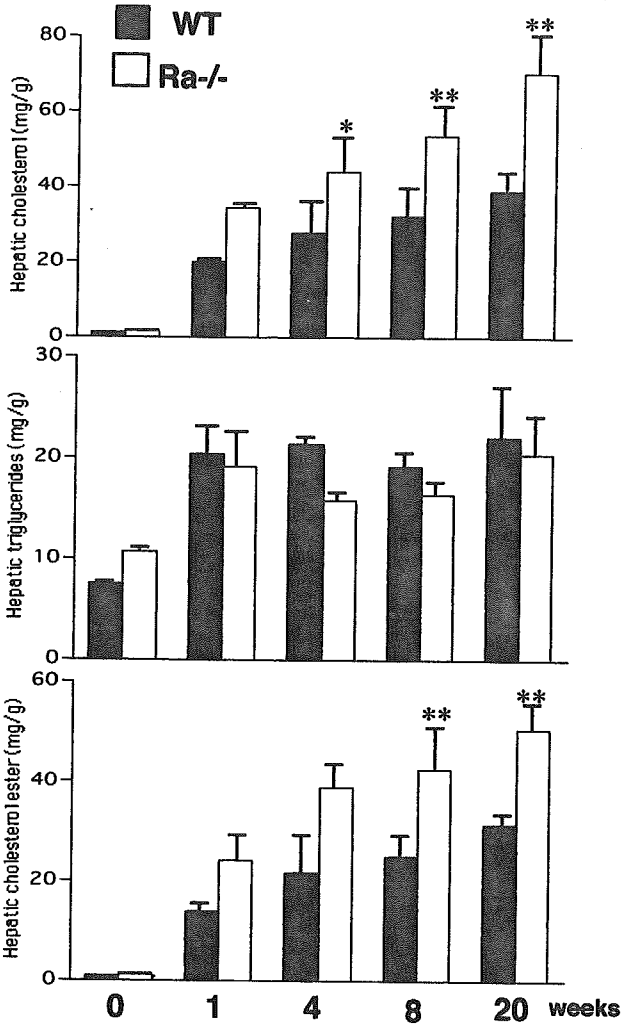

FIG. 5. **Total hepatic cholesterol, triglycerides, and cholesterol ester.** Levels of cholesterol (*upper panel*), triglycerides (*middle panel*), and cholesterol ester (*bottom panel*) content in hepatic lipid extracts of IL-1Ra$^{-/-}$ (*Ra*$^{-/-}$) and WT mice fed an atherogenic diet for 0, 1, 4, 8, or 20 weeks were measured. Levels were determined enzymatically in hepatic lipid extracts. All values are expressed as mean ± S.E. *, $p < 0.05$; **, $p < 0.01$ for IL-1Ra$^{-/-}$ mice *versus* WT mice.

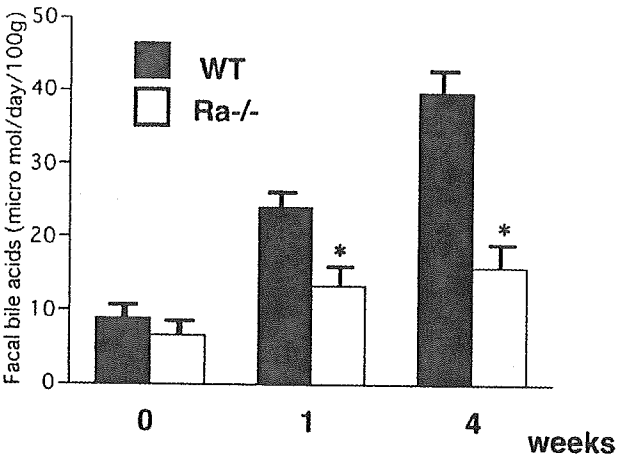

FIG. 6. **Bile acid excretion in IL-1Ra$^{-/-}$ (*Ra*$^{-/-}$) and wild type mice.** Fecal bile acid excretion in IL-1Ra$^{-/-}$ and WT mice fed an atherogenic diet for 0, 1, and 4 weeks were measured. Stool samples were collected from the mice over 72 h after 0, 1, and 4 weeks of atherogenic diet. All values are expressed as mean ± S.E. *, $p < 0.01$ for IL-1Ra$^{-/-}$ mice *versus* WT mice.

involved in acute inflammation and that cholate induces expression of genes involved in extracellular matrix deposition in hepatic fibrosis (28).

Expectedly, the levels of total cholesterol in IL-1Ra$^{-/-}$ mice were significantly higher, and the start of lipid deposition in livers of IL-1Ra$^{-/-}$ mice was observed earlier than in WT mice. These results suggest that deficiency of IL-1Ra yields abnormal lipid metabolism upon feeding on atherogenic diet. The primary route of cholesterol elimination from the body is via bile, based on both direct canalicular excretion of biliary cholesterol as well as conversion of hepatic cholesterol to bile acids (29). In our study, WT but not IL-1Ra$^{-/-}$ mice demonstrated increased bile acid excretion to maintain physiological cholesterol levels, suggesting that impairment of bile acid excretion yields significant cholesterol accumulation in response to atherogenic diet in IL-1Ra$^{-/-}$ mice.

In our study, a 2-fold increase in mRNA level of ACAT2 was observed in the IL-1Ra$^{-/-}$ mice when compared with WT mice after 4 weeks. ACAT2 is thought to function in intestinal cholesterol absorption and transport into chylomicrons as well as in providing cholesteryl esters for VLDL assembly in the liver. Indeed, ACAT2-deficient mice have reduced cholesterol absorption and are resistant to diet-induced hypercholesterolemia by a high fat, high cholesterol diet (30). Thus, the increased mRNA level of ACAT2 in IL-1Ra$^{-/-}$ mice might contribute to the hypercholesterolemia and the accumulation of lipids in the liver.

Another interesting finding in this study is that the deficiency of IL-1Ra enhances both SHP and LRH-1 mRNA expression and decreases CYP7A1 transcript in mice fed an atherogenic diet. The flux of bile acids is tightly controlled by nuclear receptors. When hepatic cholesterol levels are high, oxysterols accumulate and activate nuclear liver X-receptors, which stimulate transcription of CYP7A1 (31, 32), eventually resulting in increased bile acid synthesis and subsequent excretion of cholesterol. When bile acid levels are high, bile acid synthesis is inhibited through a regulatory cascade based on farnesoid X-receptor, SHP, and LRH-1 (33, 34). Since SHP is a particularly potent inhibitor of LRH-1 function and LRH-1 is essential for CYP7A1 expression, SHP induction results in decreased CYP7A1 expression, as confirmed *in vivo* using SHP null mice (35, 36). In the present study, levels of LRH-1 in IL-1Ra$^{-/-}$ mice were lower when compared with WT mice at basal level. The reduction of LRH-1 might be caused by chronic inflammation due to the lack of IL-1Ra, in accord with a recent report showing independently reduced LRH-1 expression during inflammation (37). The decrease of LRH-1, in turn, might suppress expression of CYP7A1 at the basal level. However, levels of LRH-1 in IL-1Ra$^{-/-}$ mice significantly increased when compared with WT mice at 4 weeks. This change might be induced by the cholestasis of IL-1Ra$^{-/-}$ mice since Bohan *et al.* (38) reported that cytokine-dependent up-regulation of LRH-1 was detected after bile duct ligation in the rat.

Several previous reports demonstrated that administration of cholic acid in mice induced *SHP* gene expression (33, 34) and that SHP reduces *CYP7A1* expression (38). Increased bile acids in the liver could, in turn, induce inflammation, and the lack of IL-1Ra, an anti-inflammatory cytokine, might deteriorate inflammation in IL-1Ra$^{-/-}$ liver. Furthermore, a large amount of cytokines induced by severe inflammation in IL-1Ra$^{-/-}$ mice could also play an important role in the up-regulation of SHP. Cytokine-dependent signaling leads to the activation of c-Jun N-terminal kinase (JNK) and other mitogen-activated protein kinases (39, 40). Recently, Gupta *et al.* (41) showed that c-Jun activated by cytokines induces *SHP* promoter activity and mutations in the AP-1 binding

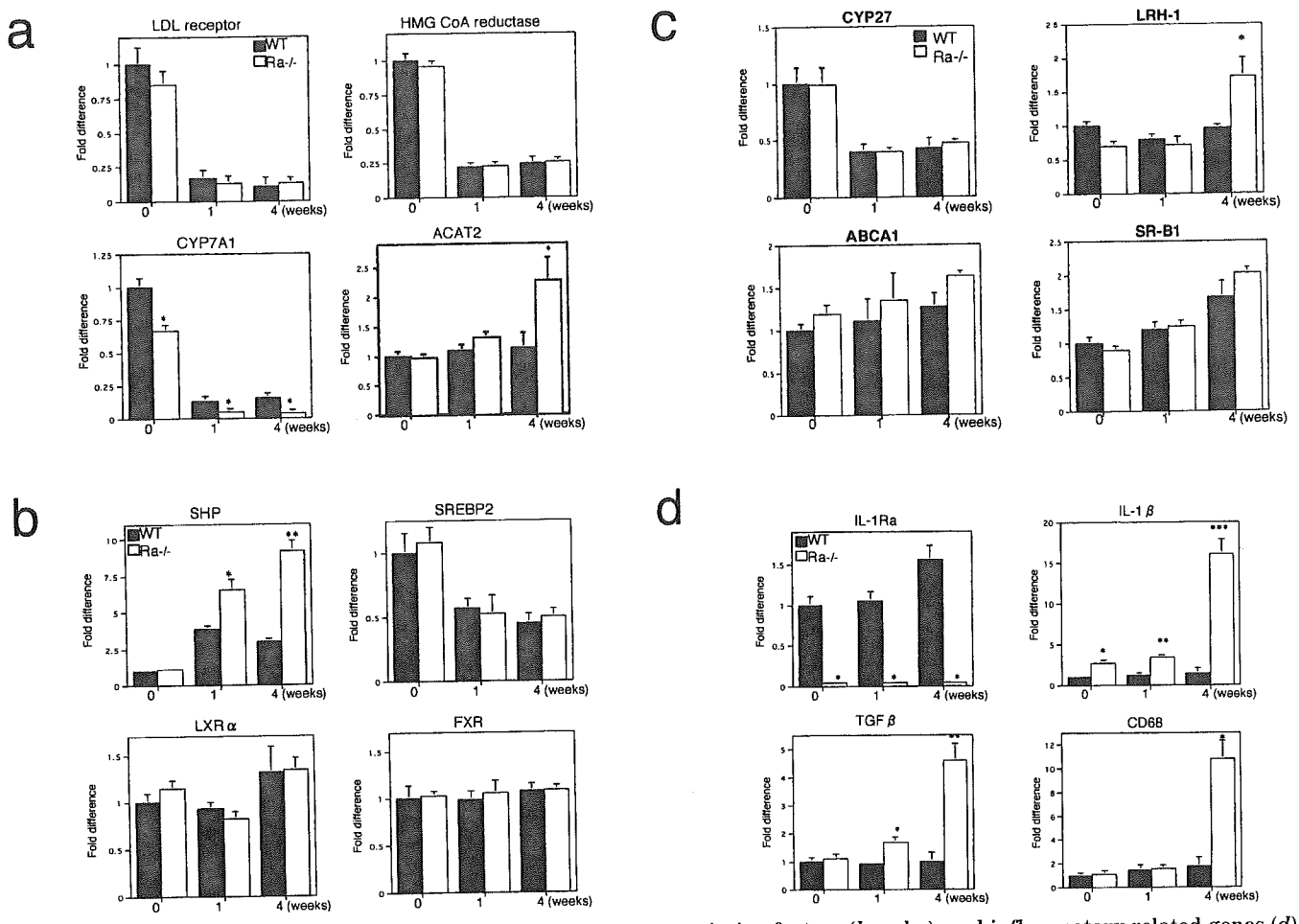

FIG. 7. **Expression of genes involved in lipid metabolism (*a*), transcription factors (*b* and *c*), and inflammatory-related genes (*d*) in the livers of IL-1Ra$^{-/-}$ (*Ra*$^{-/-}$) and wild type mice.** The mRNA levels of the indicated genes in the livers of IL-1Ra$^{-/-}$ and WT mice were quantified using real-time PCR with SYBR-green detection after 0, 1, and 4 weeks of atherogenic diet. Degree of change in gene expression is based on the day 0 baseline expression level of WT mice. All values are expressed as mean ± S.E. *, $p < 0.05$; **, $p < 0.01$, and ***, $p < 0.001$ for IL-1Ra$^{-/-}$ mice *versus* WT mice. *LXRα*, nuclear liver X-receptor α; *FXR*, farnesoid X-receptor; *TGF*, transforming growth factor.

site abolished bile acid responsiveness of the rat *SHP* promoter. Thus, they suggested that activation of the JNK/c-Jun pathway is needed for the induction of SHP by bile acids. Furthermore, Miyake *et al.* (42) demonstrated that bile acid induction of cytokine expression (such as tumor necrosis factor-α and IL-1) by macrophages correlates with repression of hepatic CYP7A1, further supporting our findings. Thus, atherogenic diet-induced inflammation under both high IL-1 levels and deficiency of IL-1Ra caused up-regulation of SHP and, in turn, down-regulation of CYP7A1. The suppression of CYP7A1 accumulates more cholesterol of IL-1Ra$^{-/-}$ mice. We conclude that the significant increase in SHP expression in IL-1Ra$^{-/-}$ liver is an indirect effect of IL-1Ra deletion, but IL-1Ra plays an important role in maintaining the cholesterol homeostasis under cholic acid-induced inflammation.

Cholesterol conversion to bile acids occurs via two different pathways: the classic and the alternative pathway. The classic pathway begins with the rate-limiting enzyme CYP7A1 (43, 44). After 1 and 4 weeks of the atherogenic diet, the expression of CYP7A1 mRNA decreased in both types of mice. However, the levels in IL-1Ra$^{-/-}$ mice were markedly lower than those in the WT mice, suggesting that the function of bile acid biosynthesis in IL-1Ra$^{-/-}$ mice was significantly attenuated following only 1 week of atherogenic diet. Our findings are in accord with a previous study that demonstrated lipopolysaccharide and cytokines resulted in a marked and very rapid decrease in CYP7A1 activity and mRNA levels (45). In contrast, differences in hepatic expression of LDL receptor and HMG-CoA reductase were not observed between IL-1Ra$^{-/-}$ and WT mice. All these data suggest that hypercholesterolemia and accumulation of lipids in IL-1Ra$^{-/-}$ mice is mainly caused by attenuation of cholesterol excretion from the liver by SHP-induced CYP7A1 suppression. However, neither the suppression of LDL receptor nor the up-regulation of HMG-CoA reductase implicated phenotype.

The decrease in HDL-cholesterol levels in IL-1Ra$^{-/-}$ mice is also in accord with the changes known to be caused by changes of ABCA1 and SR-BI in the acute phase response (17). However, no differences were observed between IL-1Ra$^{-/-}$ and WT mice in hepatic expression of ABCA1 and SR-BI, suggesting that neither ABCA1 nor SR-BI contributes to the decrease of HDL-cholesterol in IL-1Ra$^{-/-}$ mice. We think other factors, such as secretary phospholipase A_2, endothelial lipase, and lecithin cholesterol acyltransferase, may affect the decrease of HDL-cholesterol in IL-1Ra$^{-/-}$ mice. Indeed, secretory phospholipase A_2 and endothelial lipase, which hydrolyze phospholipids in HDL-cholesterol, are induced and lecithin cholesterol acyltransferase, which esterifies HDL-cholesterol, is reduced during inflammation (46–48).

Recently, Devlin *et al.* (49) showed that IL-1Ra knock-out C57BL mice fed a cholesterol/cholate diet for 3 months had a 3-fold decrease in non-HDL cholesterol when compared with WT littermate controls. However, this study did not detect differences in bilirubin levels between IL-1Ra knock-out and WT mice, whereas ALT levels were reduced. Their results

differ from our results, and the study did not demonstrate why IL-1Ra knock-out mice are protected from cholate-induced inflammation. Furthermore, their work did not analyze the mechanisms responsible for the change of cholesterol metabolism. In our study, cholesterol/cholate diet induced inflammation in the liver as reported previously (15), and the inflammation increased serum lipid levels in our mice. We think these results are in agreement with previous reports that showed that inflammation could change lipid metabolism (16, 17). Moreover, we uncovered the mechanisms of why the deficiency of IL-1Ra deteriorated cholesterol metabolism. Thus, we demonstrated for the first time that IL-1Ra plays an important role in the prevention of both fatty liver and hypercholesterolemia under inflammatory conditions.

In conclusion, deficiency of IL-1Ra deteriorated fatty liver development and cholesterol metabolism under atherogenic diet. Our results show that high cytokine levels in IL-1Ra$^{-/-}$ mice reduced mRNA expression of CYP7A1 with concurrent up-regulation of SHP mRNA expression. We conclude that IL-1Ra plays an important role in maintaining the cholesterol homeostasis under inflammatory conditions induced by cholic acid.

Acknowledgment—We thank Norbert Gerdes (Department of Medicine, the Brigham and Women's Hospital, Boston, MA) for critical review of the manuscript.

REFERENCES

1. Laskin, D. L., Weinberger, B., and Laskin, J. D. (2001) *J. Leukocyte Biol.* **70,** 163–170
2. Diehl, A. M. (2000) *Immunol. Rev.* **174,** 160–171
3. Tilg, H., and Diehl, A. M. (2000) *N. Engl. J. Med.* **343,** 1467–1476
4. Fan, J. G., Xu, Z. J., Wang, G. L., Ding, X. D., Tian, L. Y., and Zheng, X. Y. (2003) *Zhonghua Gan. Zang. Bing. Za. Zhi.* **11,** 73–76
5. McClain, C. J., Barve, S., Deaciuc, I., Kugelmas, M., and Hill, D. (1999) *Semin. Liver Dis.* **19,** 205–219
6. Thurman, R. G, Bradford, B. U., Iimuro, Y., Frankenberg, M. V., Knecht, K. T., Connor, H. D., Adachi, Y., Wall, C., Arteel, G. E., Raleigh, J. A., Forman, D. T., and Mason, R. P. (1999) *Front. Biosci.* **4,** e42–e46
7. Dinarello, C. A. (1998) *Int. Rev. Immunol.* **16,** 457–499
8. Dinarello, C. A. (2000) *N. Engl. J. Med.* **343,** 732–734
9. Gabay, C., Gigley, J., Sipe, J., Arend, W. P., and Fantuzzi, G. (2001) *Eur. J. Immunol.* **31,** 490–499
10. Matsuki, T., Horai, R., Sudo, K., and Iwakura, Y. (2003) *J. Exp. Med.* **198,** 877–888
11. Thompson, J. S. (1969) *J. Atheroscler. Res.* **10,** 113–122
12. Vesselinovitch, D., and Wissler, R. W. (1968) *J. Atheroscler. Res.* **8,** 497–523
13. Paigen, B., Morrow, A., Brandon, C., Mitchell, D., and Holmes, P. (1985) *Atherosclerosis* **57,** 65–73
14. Paigen, B., Mitchell, D., Reue, K., Morrow, A., Lusis, A. J., and Leboeuf, R. C. (1987) Proc. *Natl. Acad. Sci. U. S. A.* **84,** 3763–3767
15. Liao, F., Andalibi, A., deBeer, F. C., Fogelman, A. M., and Lusis, A. J. (1993) *J. Clin. Investig.* **91,** 2572–2579
16. Hardardottir, I., Grunfeld, C., and Feingold, K. R. (1994) *Curr. Opin. Lipidol.* **5,** 207–215
17. Khovidhunkit, W., Kim, MS., Memon, R. A., Shigenaga, J. K., Moser, A. H., Feingold, K. R., and Grunfeld, C. (2004) *J. Lipid Res.* **45,** 1169–1196
18. Macliewicz, A., Kushner, I., and Baumann, H. (1993) *Acute Phase Proteins, Molecular Biology, Biochemistry and Clinical Applications*, CRC Press, Inc., Boca Raton, FL
19. Horai, R., Asano, M., Sudo, K., Kanuka, H., Suzuki, M., Nishihara, M., Takahashi, M., and Iwakura, Y. (1998) *J. Exp. Med.* **187,** 1463–1475
20. Hedrick, C. C., Castellani, L. W., Warden, C. H., Puppione, D. L., and Lusis, A. J. (1993) *J. Biol. Chem.* **268,** 20676–20682
21. Usui, S., Hara, Y., Hosaki, S., and Okazaki, M. (2002) *J. Lipid Res.* **43,** 805–814
22. Okazaki, M., Usui, S., and Hosaki, S. (2000) in *Handbook of Lipoprotein Testing* (Rifai, N., Warnick, G. R., and Dominiczak, M. H., eds) Second Ed., pp. 647–669, American Association of Clinical Chemistry Press, Washington, D. C.
23. Folch, J., Lees, M., and Sloane Stanley, G. H. (1957) *J. Biol. Chem.* **226,** 497–509
24. Porter, J. L., Fordtran, J. S., Santa Ana, C. A., Emmett, M., Hagey, L. R., Macdonald, E. A., and Hofmann, A. F. (2003) *J. Lab. Clin. Med.* **141,** 411–418
25. Memon, R. A., Moser, A. H., Shigenaga, J. K., Grunfeld, C., and Feingold, K. R. (2001) *J. Biol. Chem.* **276,** 30118–30126
26. Baroni, G. S., D'Ambrosio, L., Curto, P., Casini, A., Mancini, R., Jezequel, A. M., and Benedetti, A. (1996) *Hepatology* **23,** 1189–1199
27. Boros, D. L., and Whitfield, J. R. (1999) *Infect. Immun.* **67,** 1187–1193
28. Vergnes, L., Phan, J., Strauss, M., Tafuri, S., and Reue, K. (2003) *J. Biol. Chem.* **278,** 42774–42784
29. Vlahcevic, Z. R., Stravitz, R. T., Heuman, D. M., Hylemon, P. B., and Pandak, W. M. (1997) *Gastroenterology* **113,** 1949–1957
30. Buhman, K. F., Accad, M., Novak, S., Choi, R. S., Wong, J. S., Homilton, R. L., Turley, S., and Farese, R. V. (2000) *Nat. Med.* **6,** 1341–1347
31. Janowski, B. A., Willy, P. J., Devi, T. R., Falck, J. R., and Mangelsdorf, D. J. (1996) *Nature* **383,** 728–731
32. Lehmann, J. M., Kliewer, S. A., Moore, L. B., Smith-Oliver, T. A., Oliver, B. B., Su, J. L., Sundseth, S. S., Winegar, D. A., Blanchard, D. E., Spencer, T. A., and Willson, T. M. (1997) *J. Biol. Chem.* **272,** 3137–3140
33. Lu, T. T., Makishima, M., Repa, J. J., Schoonjans, K., Kerr, T. A., Auwerx, J., and Mangelsdorf, D. J. (2000) *Mol. Cell.* **6,** 507–515
34. Goodwin, B., Jones, S. A., Price, R. R., Watson, M. A., McKee, D. D., Moore, L. B., Galardi, C., Wilson, J. G., Lewis, M. C., Roth, M. E., Maloney, P. R., Willson, T. M., and Kliewer, S. A. (2000) *Mol. Cell.* **6,** 517–526
35. Wang, L., Lee, Y. K., Bundman, D., Han, Y., Thevananther, S., Kim, C. S., Chua, S. S., Wei, P., Heyman, R. A., Karin, M., and Moore, D. D. (2002) *Dev. Cell.* **2,** 721–731
36. Kerr, T. A., Saeki, S., Schneider, M., Schaefer, K., Berdy, S., Redder, T., Shan, B., Russell, D. W., and Schwarz, M. (2002) *Dev. Cell.* **2,** 713–720
37. Kim, M. S., Shigenaga, J., Moser, A., Feingold, K., and Grunfeld, C. (2003) *J. Biol. Chem.* **278,** 8988–8995
38. Bohan, A., Chen, WS., Denson, L. A., Held, M. A., and Boyer, J. L. (2003) *J. Biol. Chem.* **278,** 36688–36698
39. Li, X., Commane, M., Burns, C., Vithalani, K., Cao, Z., and Stark, G. R. (1999) Mol. *Cell. Biol.* **19,** 4643–4652
40. Lomaga, M. A., Yeh, W. C., Sarosi, I., Duncan, G. S., Furlonger, C., Ho, A., Morony, S., Capparelli, C., Van, G., Kaufman, S., van der Heiden, A., Itie, A., Wakeham, A., Khoo, W., Sasaki, T., Cao, Z., Penninger, J. M., Paige, C. J., Lacey, D. L., Dunstan, C. R., Boyle, W. J., Goeddel, D. V., and Mak, T. W. (1999) *Genes Dev.* **13,** 1015–1024
41. Gupta, S., Stravitz, R. T., Dent, P., and Hylemon, P. B. (2001) *J. Biol. Chem.* **276,** 15816–15822
42. Miyake, J. H., Wang, S-L., and Davis, R. A. (2000) *J. Biol. Chem.* **275,** 21805–21808
43. Chiang, J. Y. L. (1998) *Front. Biosci.* **3,** D176–D193
44. Schwarz, M., Lund, E. G., and Russell, D. W. (1998) *Curr. Opin. Lipidol.* **9,** 113–118
45. Feingold, K. R., Spady, D. K., Pollock, A. S., Moser, A. H., and Grunfeld, C. (1996) *J. Lipid Res.* **37,** 223–228
46. Pruzanski, W., Vadas, P., and Browning, J. (1993) *J. Lipid. Mediat.* **8,** 161–167
47. Jin, W., Sun, G. S., Marchadier, D., Octtaviani, E., Glick, J. M., and Rader, D. J. (2003) *Circ. Res.* **92,** 644–650
48. Ly, H., Francone, O. L., Fielding, C. J., Shigenaga, J. K., Moser, A. H., Grunfeld, C., and Feingold, K. R. (1995) *J. Lipid Res.* **36,** 1254–1263
49. Devlin, C. M., Kuriakose, G., Hirsch, E., and Tabas, I. (2002) *Proc. Natl. Acad. Sci. U. S. A.* **99,** 6280–6285

JEM

BRIEF DEFINITVE REPORT

Dok-1 and Dok-2 are negative regulators of lipopolysaccharide-induced signaling

Hisaaki Shinohara,[1,2] Akane Inoue,[1] Noriko Toyama-Sorimachi,[3] Yoshinori Nagai,[4] Tomoharu Yasuda,[1] Hiromi Suzuki,[5] Reiko Horai,[6] Yoichiro Iwakura,[6] Tadashi Yamamoto,[5] Hajime Karasuyama,[3] Kensuke Miyake,[4] and Yuji Yamanashi[1,2]

[1]Department of Cell Regulation, Medical Research Institute, [2]School of Biomedical Science, and [3]Department of Immune Regulation, Graduate School, Tokyo Medical and Dental University, Tokyo 113-8510, Japan
[4]Division of Infectious Genetics, [5]Department of Oncology, and [6]Center for Experimental Medicine, Institute of Medical Science, University of Tokyo, Tokyo 108-8639, Japan

Endotoxin, a bacterial lipopolysaccharide (LPS), causes fatal septic shock via Toll-like receptor (TLR)4 on effector cells of innate immunity like macrophages, where it activates nuclear factor κB (NF-κB) and mitogen-activated protein (MAP) kinases to induce proinflammatory cytokines such as tumor necrosis factor (TNF)-α. Dok-1 and Dok-2 are adaptor proteins that negatively regulate Ras–Erk signaling downstream of protein tyrosine kinases (PTKs). Here, we demonstrate that LPS rapidly induced the tyrosine phosphorylation and adaptor function of these proteins. The stimulation with LPS of macrophages from mice lacking Dok-1 or Dok-2 induced elevated Erk activation, but not the other MAP kinases or NF-κB, resulting in hyperproduction of TNF-α and nitric oxide. Furthermore, the mutant mice showed hyperproduction of TNF-α and hypersensitivity to LPS. However, macrophages from these mutant mice reacted normally to other pathogenic molecules, CpG oligodeoxynucleotides, poly(I:C) ribonucleotides, or Pam_3CSK_4 lipopeptide, which activated cognate TLRs but induced no tyrosine phosphorylation of Dok-1 or Dok-2. Forced expression of either adaptor, but not a mutant having a Tyr/Phe substitution, in macrophages inhibited LPS-induced Erk activation and TNF-α production. Thus, Dok-1 and Dok-2 are essential negative regulators downstream of TLR4, implying a novel PTK-dependent pathway in innate immunity.

CORRESPONDENCE
Yuji Yamanashi:
yamanashi.creg@mri.tmd.ac.jp

The innate immune response to microbial pathogens begins when pathogen-associated molecular patterns (PAMPs) meet their cognate receptors on effector cells. PAMPs are conserved motifs on pathogens that are usually not found in higher eukaryotes and include LPS, a bacterial cell wall component and the most potent stimulator in innate immunity (1). Toll-like receptors (TLRs) recognize PAMPs, and LPS stimulates the TLR4–MD-2 receptor complex, which then triggers intracellular signaling cascades (TLR4 signaling) including the activation of NF-κB and three types of mitogen-activated protein (MAP) kinases: Erk, JNK, and p38 (2, 3). These signaling molecules play indispensable roles in inducing TNF-α, a key proinflammatory cytokine for innate immunity (4). Recent studies have revealed that another LPS receptor, CD14, facilitates the binding of LPS to the TLR4–MD-2 complex and consequent intracellular signaling (5). In addition, TLR-mediated signaling depends upon adaptor molecules such as MyD88 and Toll/IL-1 receptor domain–containing adaptor-inducing IFN-β (TRIF) and is often classified into a MyD88- or TRIF-dependent pathway. In fact, TLR4 triggers both pathways, and macrophages from mice lacking these adaptors are defective in proinflammatory responses to LPS (6).

Although the innate immune response is essential for controlling the growth of pathogenic microbes, negative regulation is also critical because excessive and unleashed responses can cause inflammatory diseases such as septic shock or chronic inflammation (4, 7–10). A Toll IL-1 receptor family protein ST2 was recently reported as an inducible negative regulator of the MyD88-dependent pathway (7). Indeed, mice lacking ST2 failed to develop endotoxin tolerance a few days after primary administra-

H. Shinohara's present address is Laboratory for Lymphocyte Differentiation, RIKEN Research Center for Allergy and Immunology, Kanagawa 230-0045, Japan.

The online version of this article contains supplemental material.

JEM © The Rockefeller University Press $8.00
Vol. 201, No. 3, February 7, 2005 333–339 www.jem.org/cgi/doi/10.1084/jem.20041817

Supplemental Material can be found at:
http://www.jem.org/cgi/content/full/jem.20041817/DC1

tion of a sublethal dose of LPS. However, due to the lag period for its induction, ST2 appeared irrelevant to primary endotoxin shock, a septic shock rapidly induced by LPS. Gene targeting studies further revealed that IL-1 receptor–associated kinase (IRAK)-M and suppressor of cytokine signaling 1 are inducible negative regulators of LPS responses (8–10). Despite these findings, very little is known about constitutively expressed negative regulator(s) of TLR4 signaling, which could work instantaneously upon LPS treatment of macrophages to control the early phase of the signaling and oppose endotoxin shock.

Dok-1 was originally identified as a major substrate of many protein tyrosine kinases (PTKs; references 11–13). When tyrosine phosphorylated, Dok-1 and its closest homologue Dok-2 work as adaptor proteins and recruit multiple SH2-containing molecules such as p120 rasGAP and Nck. These adaptors are preferentially expressed in hematopoietic cells and share structural similarities characterized by NH_2-terminal PH and PTB domains, followed by COOH-terminal SH2 target motifs (11). Experiments with mice lacking Dok-1 or Dok-2 demonstrated an indispensable role in the negative regulation of Erk downstream of PTKs in various hematopoietic cells (14–16). However, mice lacking either adaptor did not show overt defects in hematopoiesis. Although the biological significance of PTKs in TLR4 signaling is controversial, LPS activates cytoplasmic PTKs including Lyn, which is essential for the phosphorylation of Dok-1 upon B cell receptor signaling (15, 17). Here, we have studied the role of Dok-1 and Dok-2 and demonstrate that these adaptors are constitutively expressed negative regulators of TLR4 signaling.

RESULTS AND DISCUSSION

Dok-1 and Dok-2 are negative regulators of TNF-α and nitric oxide (NO) production upon LPS treatment of macrophages

To understand the role of Dok-1 and Dok-2 in TLR4 signaling, we first examined the production of two major signal mediators of innate immunity, TNF-α and NO, upon LPS treatment of macrophages from mice lacking Dok-1 or Dok-2. The peritoneal resident and BM-derived macrophages from either of the mutant mice showed a larger population of TNF-α–producing cells and greater NO production than the wild-type cells, respectively (Fig. 1, A and B). However, both mutant macrophages expressed normal levels of LPS receptors, TLR4–MD-2, and CD14, indicating that loss of Dok-1 or Dok-2 does not cause down-regulation of these receptors (Fig. S1, available at http://www.jem.org/cgi/content/full/jem.20041817/DC1). Thus, Dok-1 and Dok-2 are indispensable negative regulators of TNF-α and NO production downstream of TLR4.

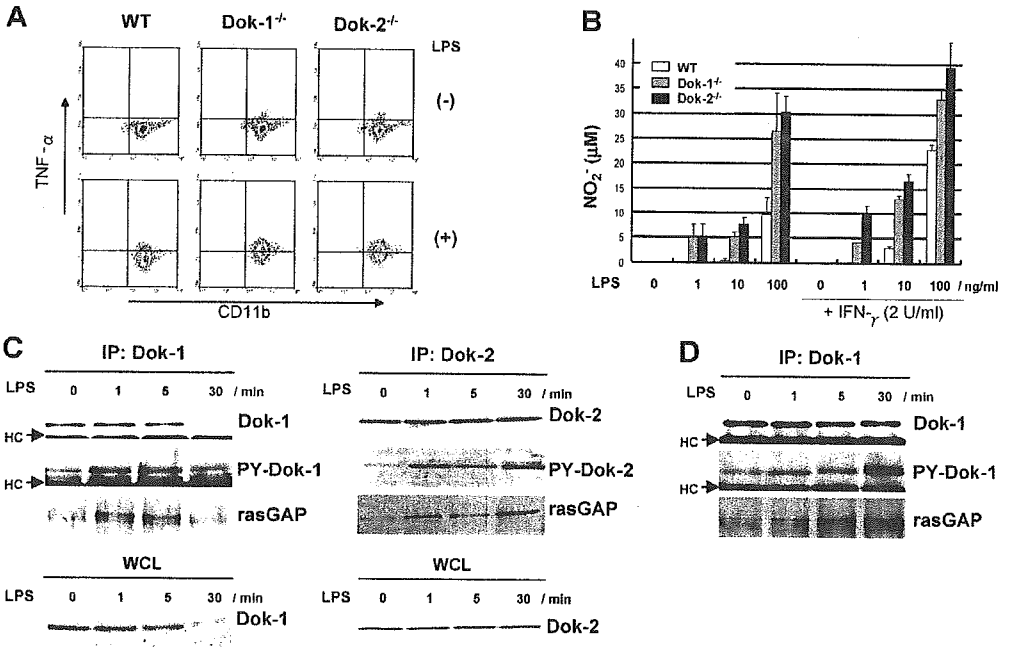

Figure 1. Dok-1 and Dok-2 are adaptors essential to the negative regulation of LPS responses. (A) Peritoneal resident macrophages from mice were treated with (+) or without (−) LPS, and then intracellular TNF-α production of $CD11b^+$ cells was examined with flow cytometry. (B) BM-derived macrophages were cultured in the indicated concentration of LPS and IFN-γ, and then NO production was evaluated. SD is from sextuplicate experiments. (C) Dok-1 or Dok2 immunoprecipitates (IP) or whole cell lysates (WCL) were subjected to immunoblotting for Dok-1, Dok-2, phosphotyrosine (PY-Dok-1 or PY-Dok-2), or p120 rasGAP upon LPS treatment of peritoneal macrophages for the indicated period. Position of immunoglobulin heavy chain (HC) is indicated. (D) Dok-1 immunoprecipitates were adjusted to contain the same levels of Dok-1 in quantity and examined as in C.

Dok-1 and Dok-2 are essential adaptors in the negative regulation of Erk upon LPS treatment

To address the molecular mechanisms of the Dok-1– and Dok-2–mediated negative regulation of LPS-evoked responses, we examined the tyrosine phosphorylation and adaptor function in peritoneal macrophages. Antiphosphotyrosine immunoblot and coimmunoprecipitation analyses revealed that the Dok family proteins were indeed tyrosine phosphorylated as early as 1 min after LPS treatment and coimmunoprecipitated with p120 rasGAP (Fig. 1 C). Interestingly, Dok-1, but not Dok-2, decreased in quantity at least 30 min after the stimulation, indicating that the biochemical responses of these proteins differ. However, when immunoprecipitated Dok-1 was adjusted to the same quantity at each time point, its tyrosine phosphorylation and binding to rasGAP was obvious even 30 min after the stimulation with LPS (Fig. 1 D). These results indicate that Dok-1 and Dok-2 are adaptors involved in LPS-evoked signaling, which activates PTK(s) to phosphorylate them, and also suggest that these adaptors negatively regulate Erk upon TLR4 signaling, like in many other signaling situations downstream of PTKs. Thus, the activation of Erk as well as JNK and p38 MAP kinase was evaluated upon LPS treatment of BM-derived macrophages from mice lacking Dok-1 or Dok-2. Although JNK and p38 MAP kinase activation was normal in those macrophages, the activation of Erk was remarkably enhanced and sustained (Fig. 2 A). In addition, the phosphorylation and degradation of IκB-α as well as the activation of

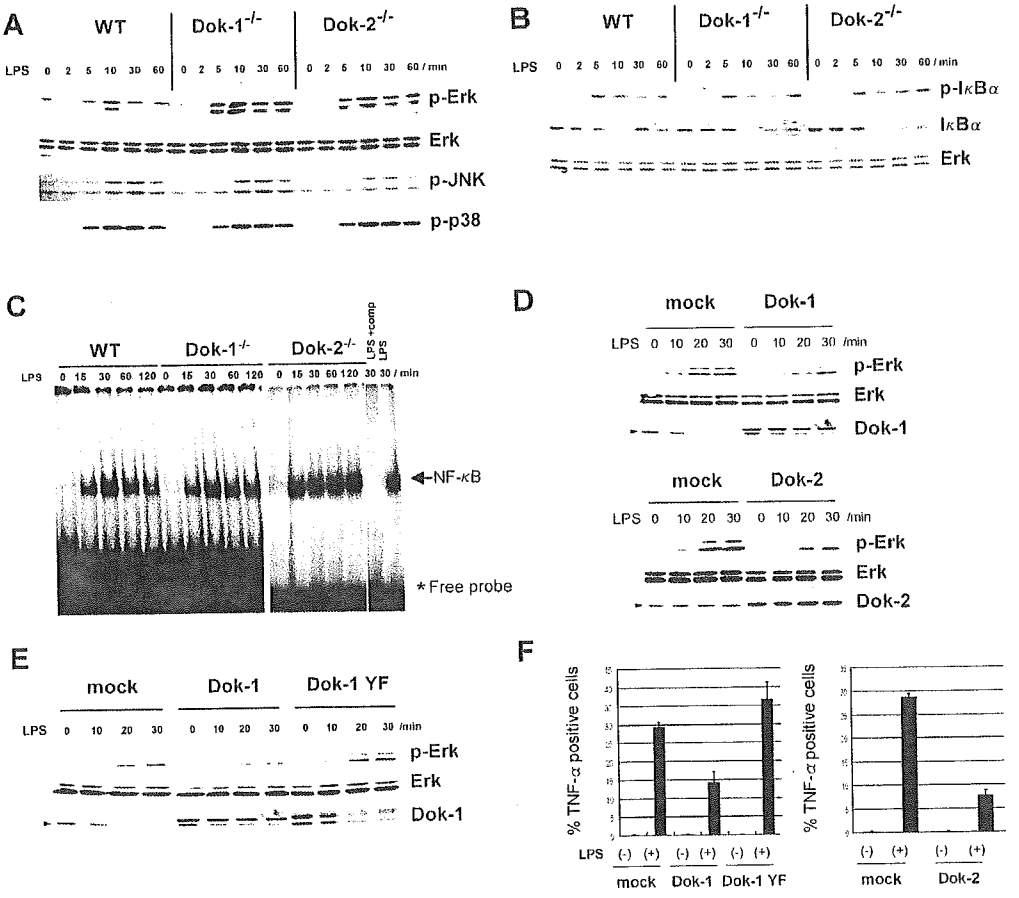

Figure 2. Dok-1 and Dok-2 are negative regulators of Erk upon TLR4 signaling. (A) Total Erk, activated Erk (p-Erk), JNK (p-JNK), or p38 MAP kinase (p-p38) was examined with immunoblotting upon LPS treatment of BM-derived macrophages from mice. (B) NF-κB activation was assessed by immunoblotting for IκBα or its phosphorylation (p-IκBα) upon LPS treatment of macrophages in A. Control immunoblotting for Erk was performed. (C) NF-κB activity was examined by gel mobility shift assay upon LPS treatment of peritoneal macrophages. Positions of the NF-κB complex and the free probes are indicated. The specificity was determined by adding excess amounts of unlabeled competitor of the probe (LPS + comp) or not (LPS) to nuclear extracts of wild-type macrophages. (D) Activated Erk (p-Erk), total Erk, Dok-1, or Dok-2 was examined with immunoblotting upon LPS treatment of RAW 264.7 cells (mock) or those expressing exogenous Dok-1 (top) or Dok-2 (bottom). An arrowhead indicates the position of endogenous Dok-1 or Dok-2. (E) RAW 264.7 cells (mock) or those expressing exogenous Dok-1 or a Dok-1 mutant (Dok-1 YF) were examined as in D. (F) RAW 264.7 cells (mock) or those expressing exogenous Dok-1, Dok-1 YF, or Dok-2 were cultured in the presence (+) or absence (−) of LPS, and then the percentage of intracellular TNF-α$^+$ cells was determined with flow cytometry. SD is from triplicate experiments.

NF-κB were unaffected in macrophages regardless of the mutations (Fig. 2, B and C). Together, our findings demonstrate that Dok-1 and Dok-2 are essential adaptors in the negative regulation of Erk, but not JNK, p38 MAP kinase, and NF-κB, upon TLR4 signaling. Moreover, that the expression levels of Dok-1 and Dok-2 were unchanged at least early on and the phosphorylation was very rapid upon LPS treatment indicates that both adaptors are on standby before the onset of the signaling to be rapidly activated (Fig. 1 C).

Forced expression of Dok-1 or Dok-2 inhibits LPS-induced Erk activation and TNF-α production

To confirm that Dok-1 and Dok-2 are negative regulators of Erk and TNF-α responses to LPS, we examined if forced expression in macrophages of either adaptor suffices to inhibit those responses. The control RAW 264.7 macrophages displayed an intact Erk activation, TNF-α production, and Dok-1 down-regulation upon LPS treatment (Fig. 2, D–F). However, forced expression of flag-tagged Dok-1 or Dok-2 clearly inhibited the Erk and TNF-α responses to LPS, indicating that Dok-1 and Dok-2 are potent negative regulators of the signaling. Note that the flag-tagged Dok-1, but not Dok-2, was down-regulated like the endogenous Dok-1. Recently, we identified Tyr-336 and Tyr-340 as essential residues for Dok-1 to inhibit the Ras–Erk pathway downstream of Lyn (18). Consistently, forced expression of a flag-tagged Dok-1 mutant having a Tyr/Phe substitution at these residues (Dok-1 YF) resulted in a loss of inhibitory effects on the LPS-evoked responses (Fig. 2, E and F). These results strongly suggest that tyrosine phosphorylation of Dok-1 and probably Dok-2 is essential for the inhibitory effects downstream of TLR4.

Although little is known about the regulation of Erk downstream of LPS, it was reported that a MAP kinase kinase kinase, Tpl2/Cot, is required for the LPS-mediated activation of Erk in macrophages (19). The authors showed that loss of Tpl2 specifically blocks the activation of Erk among MAP kinases and NF-κB and that inhibition of MEK, and thereby inhibition of Erk, suppressed TNF-α production upon LPS signaling. Moreover, it was suggested that not only LPS but also Tpl2 requires the Ras pathway to activate Erk (20, 21). Therefore, Ras appears to be an essential element for the activation of Erk downstream of TLR4. Given that the Dok-1 YF mutant lacking residues essential for the inhibition of Ras had no inhibitory effect upon TLR4 signaling (Fig. 2, E and F), the negative signaling of Dok-1 against Erk may intersect the Tpl2-mediated positive signaling in the Ras pathway downstream of TLR4. Further studies are required to understand molecular mechanisms of the Dok-1 and Dok-2 function in the TLR4 pathway, including the negative regulation of TNF-α production and interaction with their regulators and effectors.

Dok-1 and Dok-2 are irrelevant to TLR9, TLR3, or TLR2 signaling

To delineate the Dok-1 and Dok-2 function in TLR-mediated signaling, we examined their role upon the stimulation of macrophages with CpG oligodeoxynucleotide (ODN) and poly(I:C), which mimic microbial nucleotides and induce MyD88-dependent and TRIF-dependent pathways through TLR9 and TLR3, respectively. Interestingly, both nucleotides induced normal levels of Erk, JNK, and p38 MAP kinase activation as well as TNF-α production regardless of Dok-1 or Dok-2 mutation, indicating that both adaptors are dispensable to the signaling downstream of these TLRs (Fig. 3, A and B, and Fig. S2, available at http://www.jem.org/cgi/content/full/jem.20041817/DC1). Because TLR3 and TLR9 are thought to be intracellular receptors, whereas

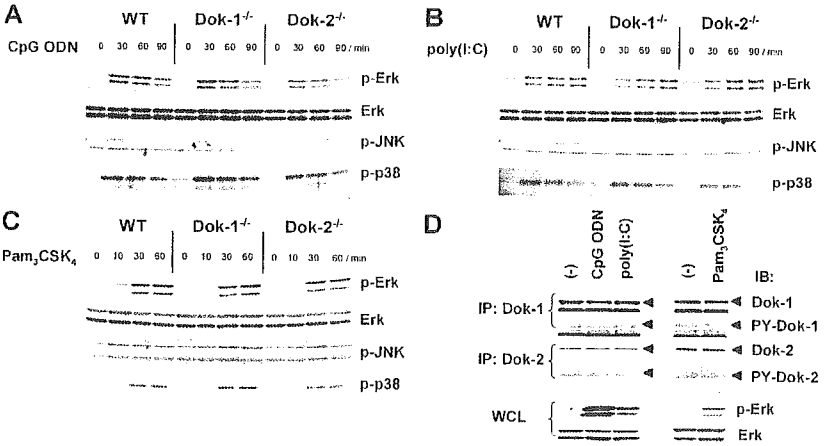

Figure 3. Dok-1 and Dok-2 are irrelevant to TLR9, TLR3, or TLR2 signaling. (A–C) Activation of each MAP kinase was examined as in Fig. 2 A upon CpG ODN, poly(I:C), or Pam_3CSK_4 treatment of BM-derived macrophages from mice. (D) Dok-1 or Dok-2 immunoprecipitates (IP) were subjected to immunoblotting (IB) for Dok-1, Dok-2, or phosphotyrosine (PY-Dok-1 or PY-Dok-2) upon CpG ODN, poly(I:C), or Pam_3CSK_4 treatment of wild-type peritoneal macrophages for 30 min. Whole cell lysates (WCL) from these macrophages were subjected to immunoblotting for activated Erk (p-Erk) or total Erk as controls.